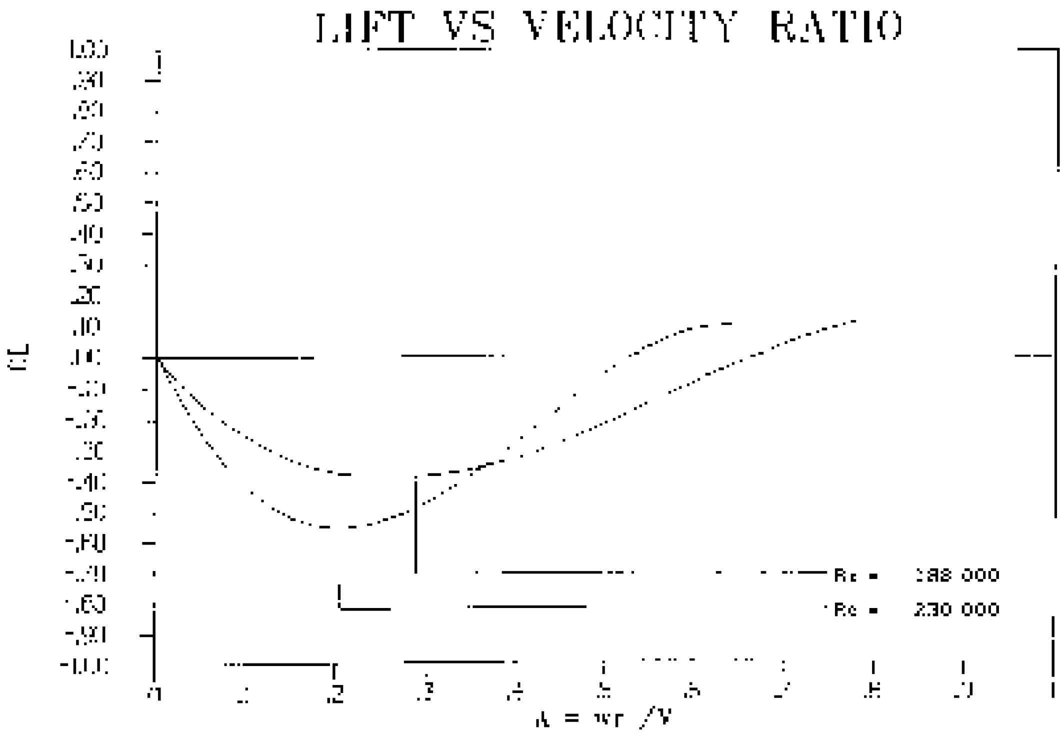

Fig 7.19. Lift vs velocity ratio with $\gamma = 90°$ for those tests using support A in position 2.

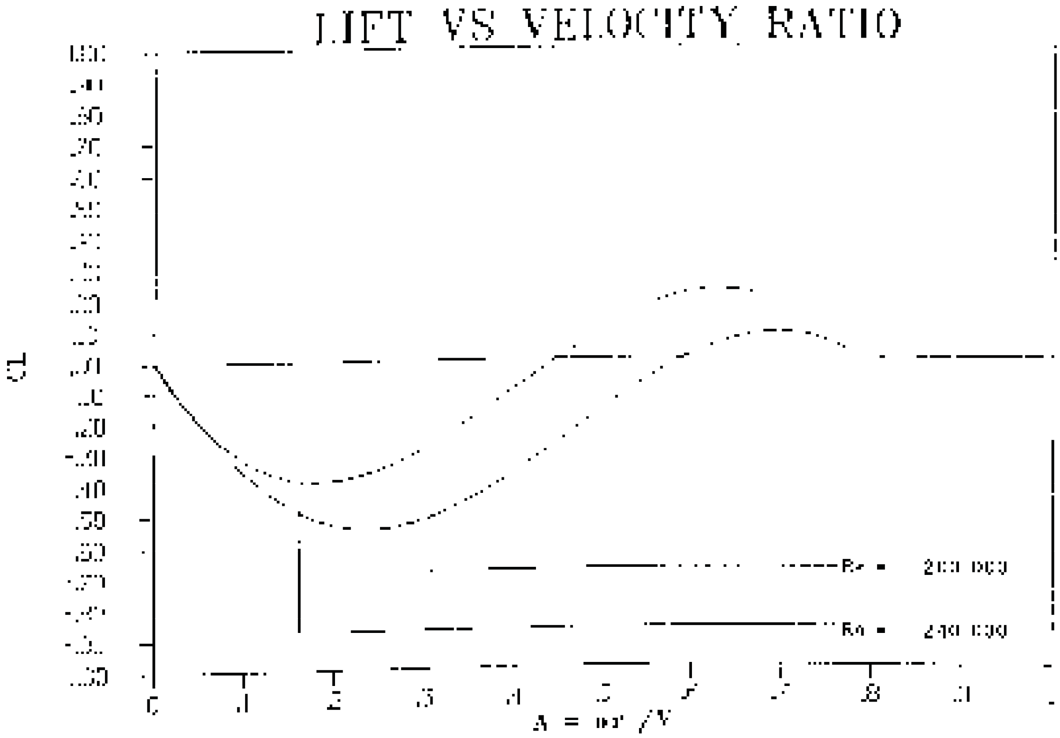

Fig 7.20. Lift vs velocity ratio with $\gamma = 90°$ for those tests using support B in position 2.

7.3 VARIATION OF DRAG WITH SPIN PARAMETER

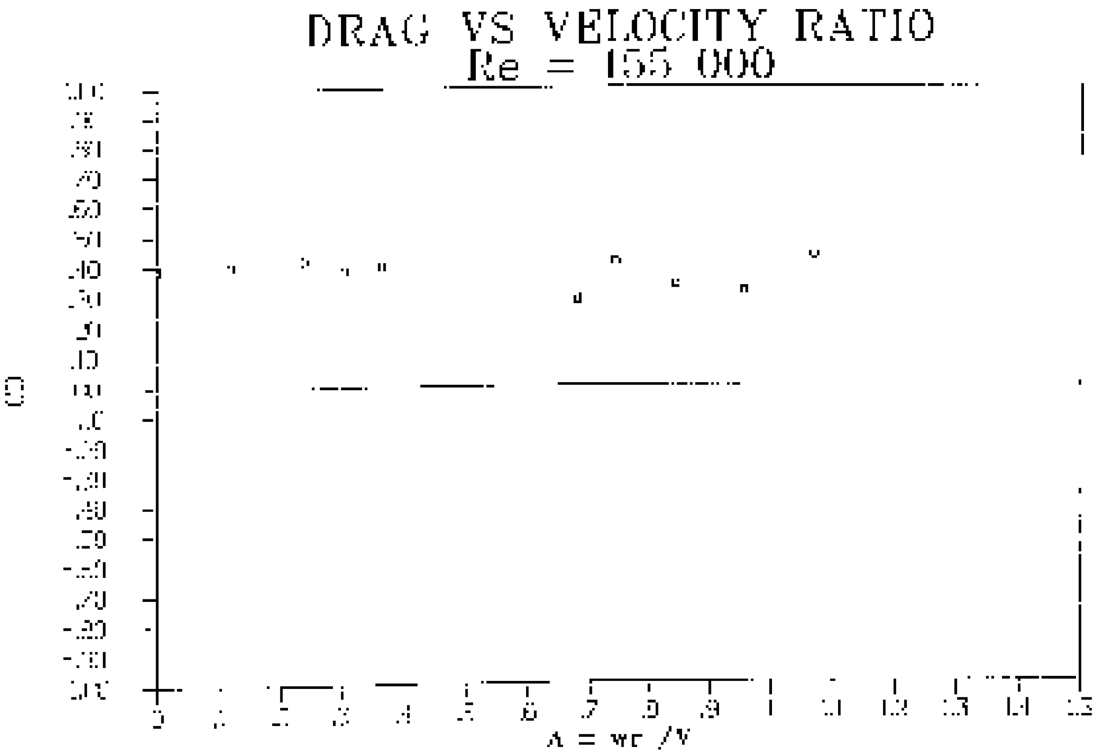

Fig 7.21. Drag vs velocity ratio for Re = 155 000 with γ = 90° using support A in position 1.

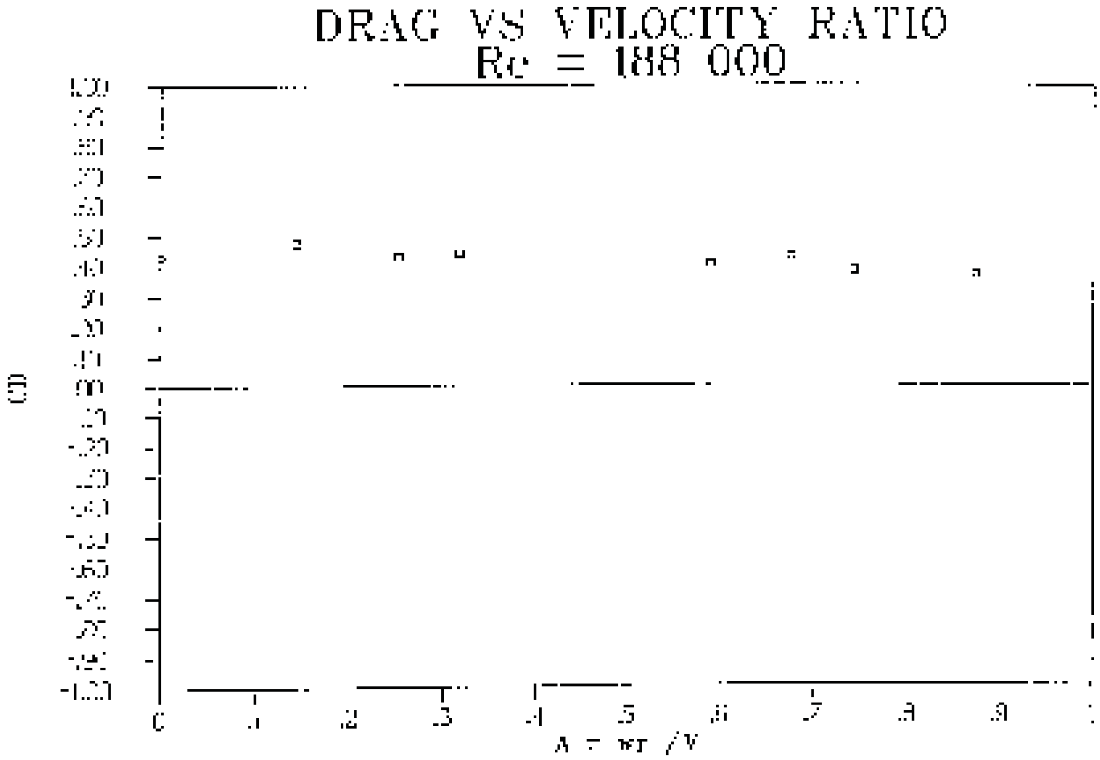

Fig 7.22. Drag vs velocity ratio for Re = 188 000 with γ = 90 ° using support A in position 1.

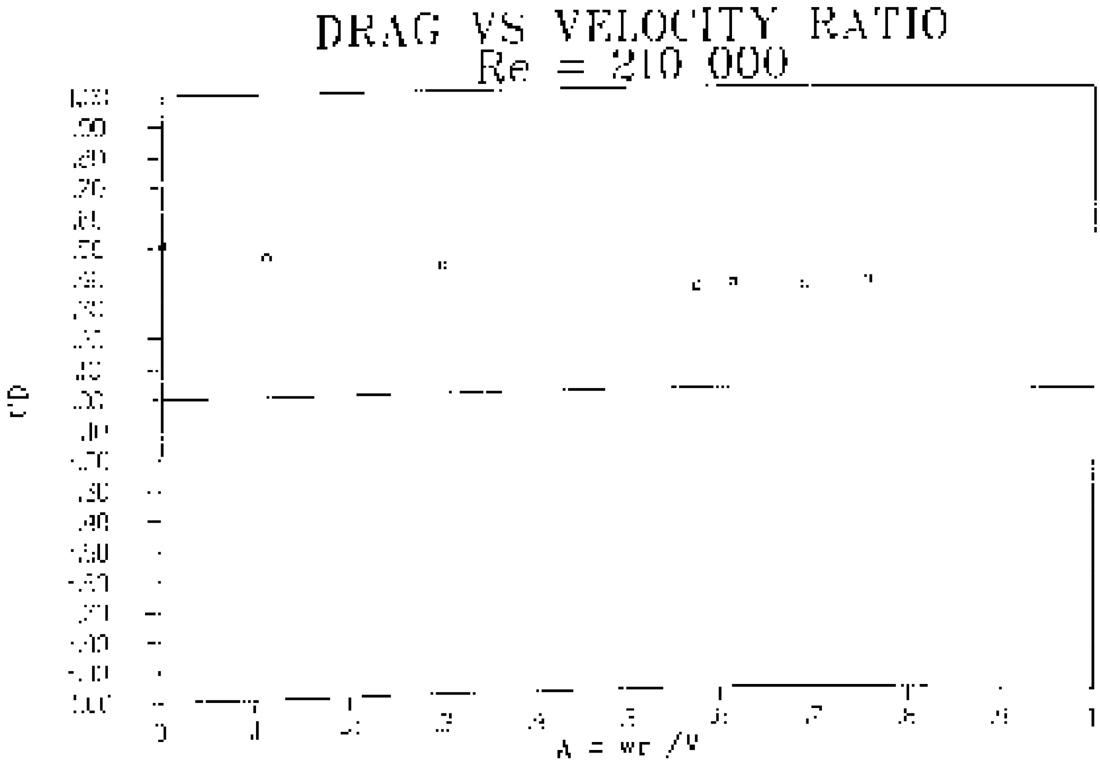

Fig 7.23. Drag vs velocity ratio for Re = 210 000 with γ = 90 ° using support A in position 1.

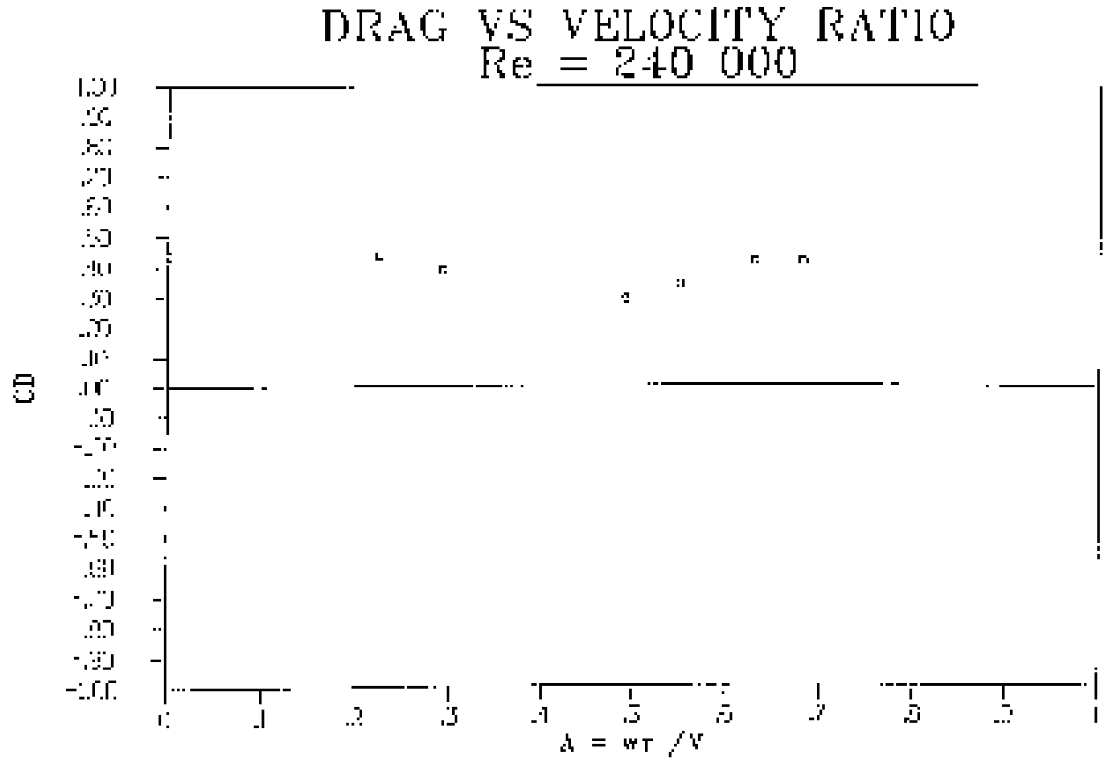

Fig 7.24. Drag vs velocity ratio for Re = 240 000 with γ = 90° using support A in position 1.

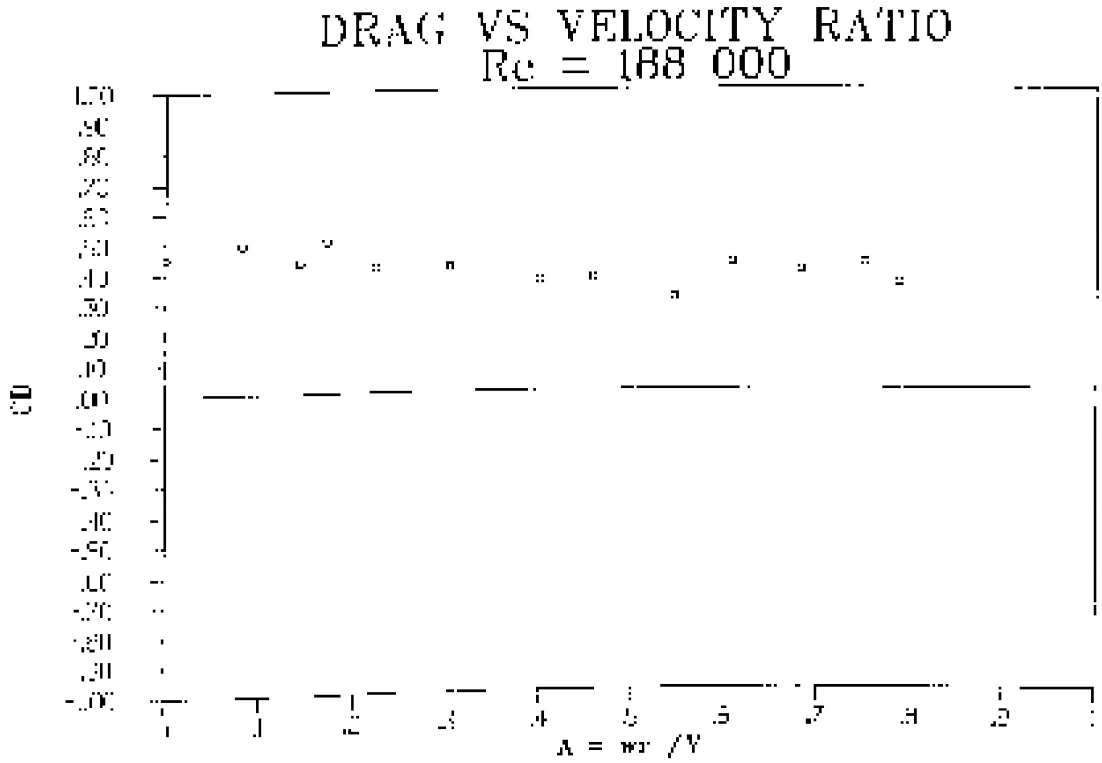

Fig 7.25. Drag vs velocity ratio for Re = 188 000 with γ = 90° using support A in position 2.

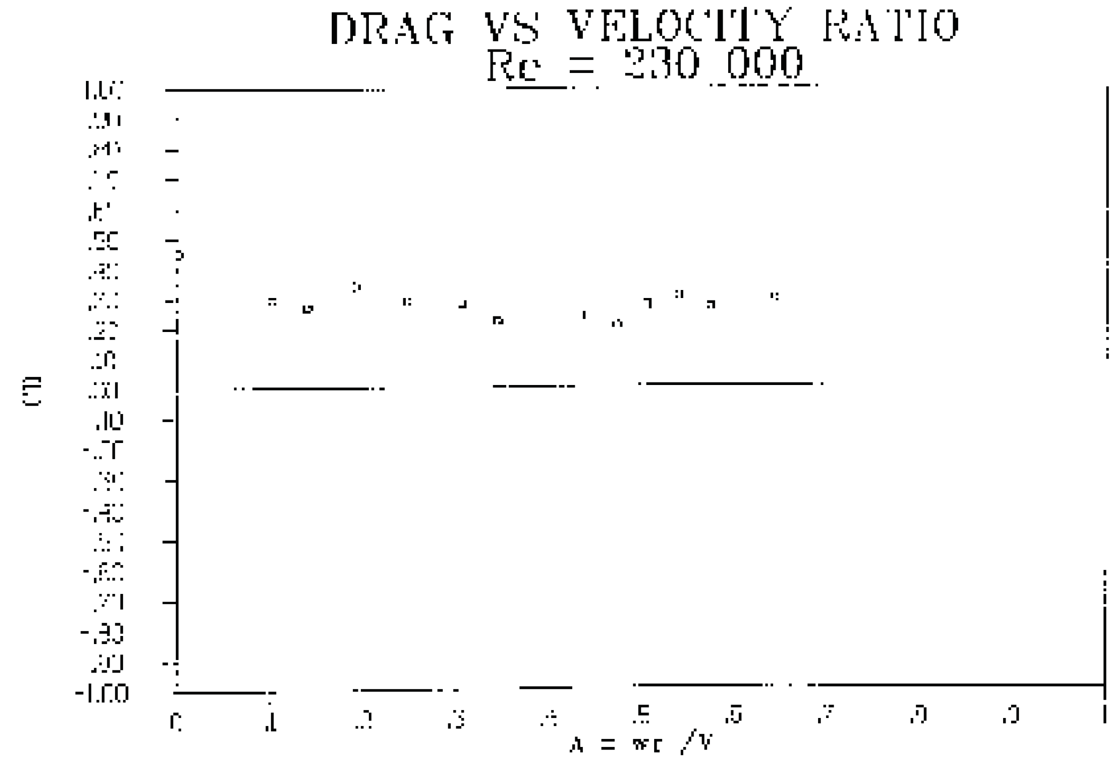

Fig 7.26. Drag vs velocity ratio for Re = 230 000 with γ = 90° using support A in position 2.

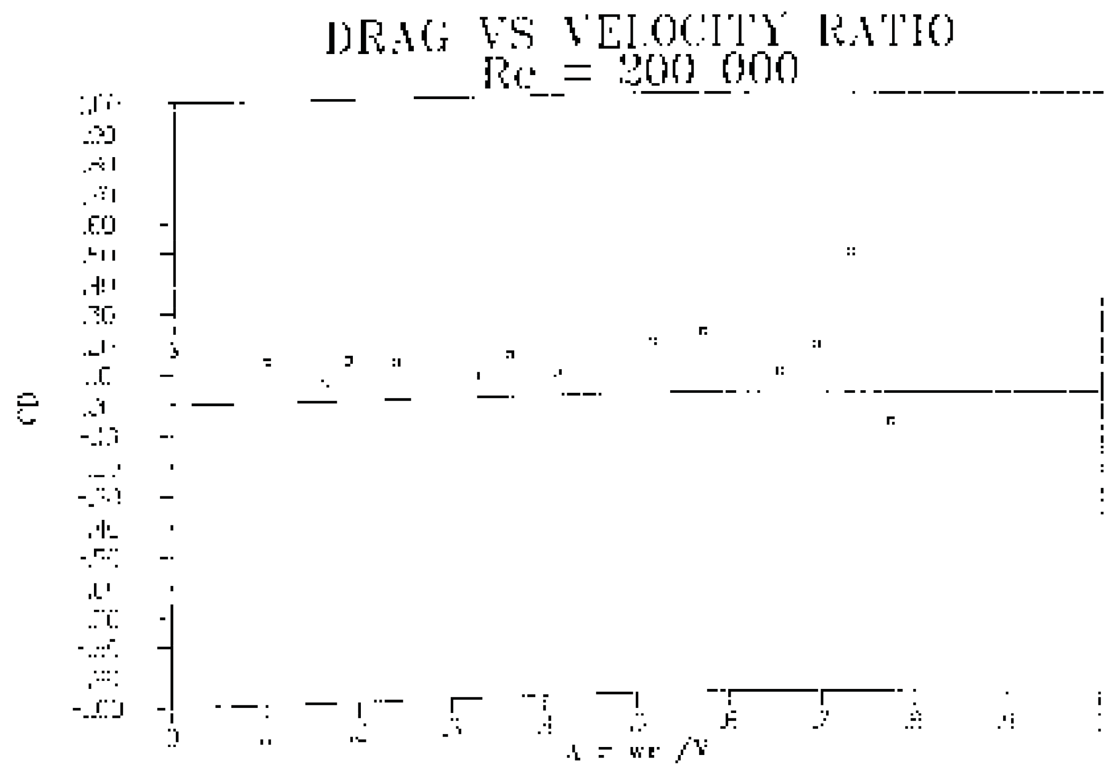

Fig 7.27. Drag vs velocity ratio for Re = 200 000 with γ = 90° using support B in position 2.

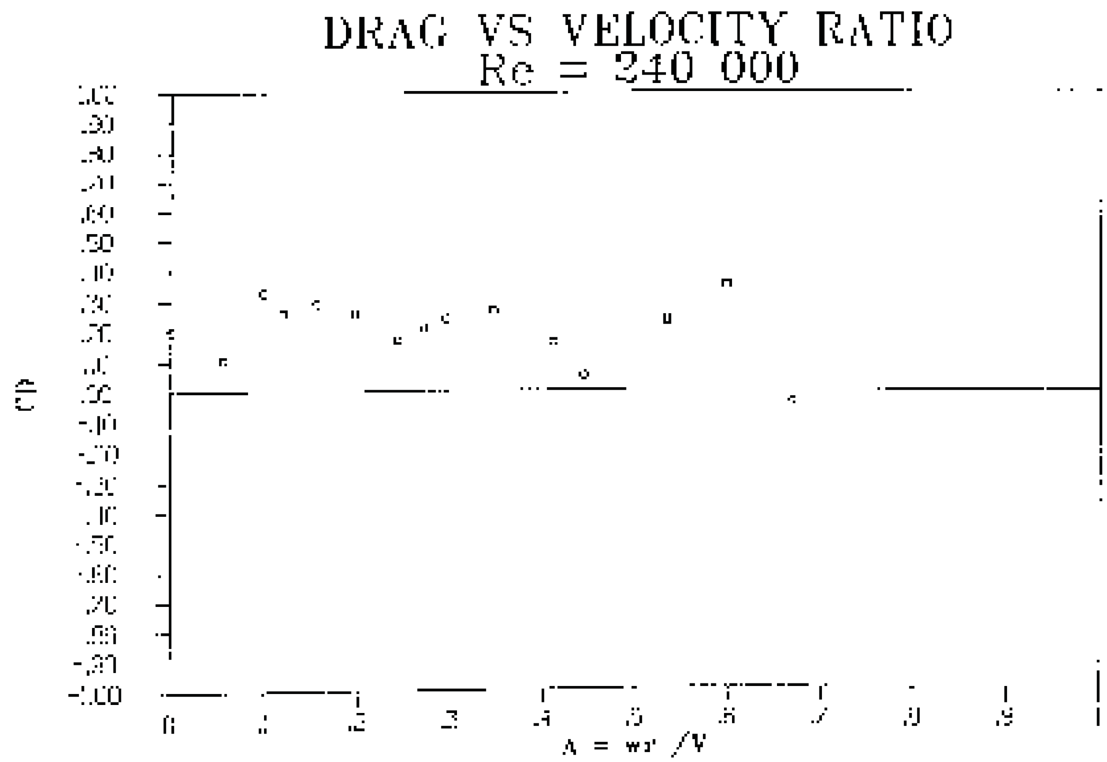

Fig 7.28. Drag vs velocity ratio for Re = 240 000 with γ = 90° using support B in position 2.

7.4 LIFT AND DRAG VARIATION WITH YAW ANGLE

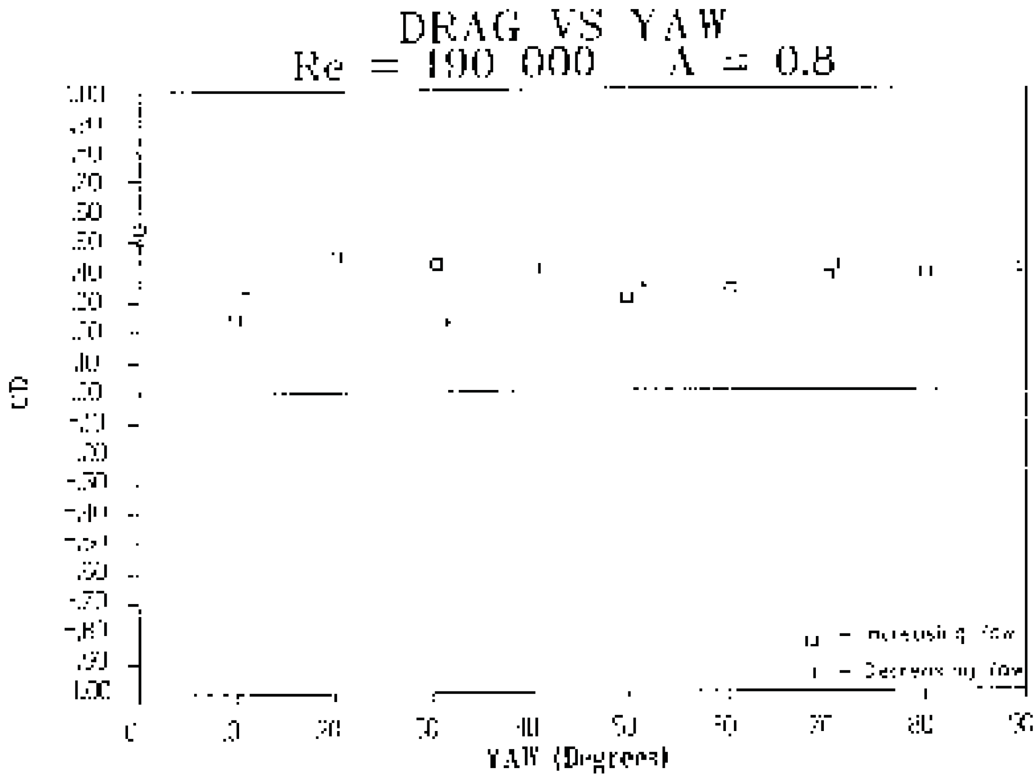

Fig 7.29. Drag vs Yaw angle for Re = 190 000 and the velocity ratio A = 0.8 using support A in position 1.

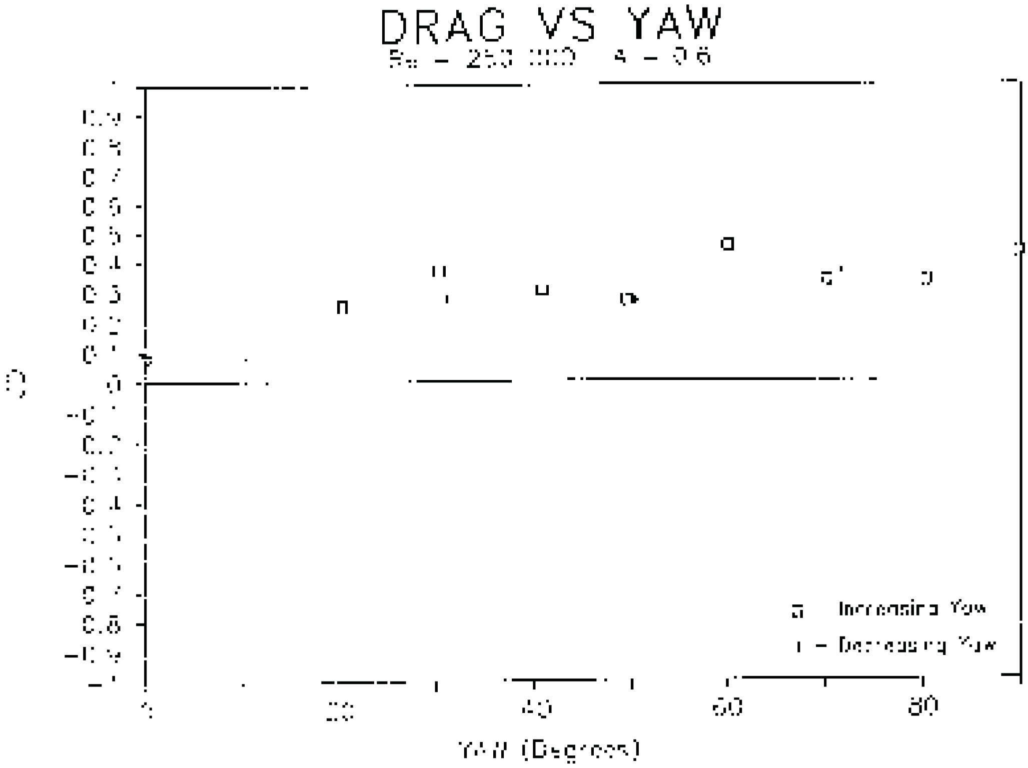

Fig 7.30. Drag vs Yaw angle for Re = 250 000 and the velocity ratio A = 0.6 using support A in position 1.

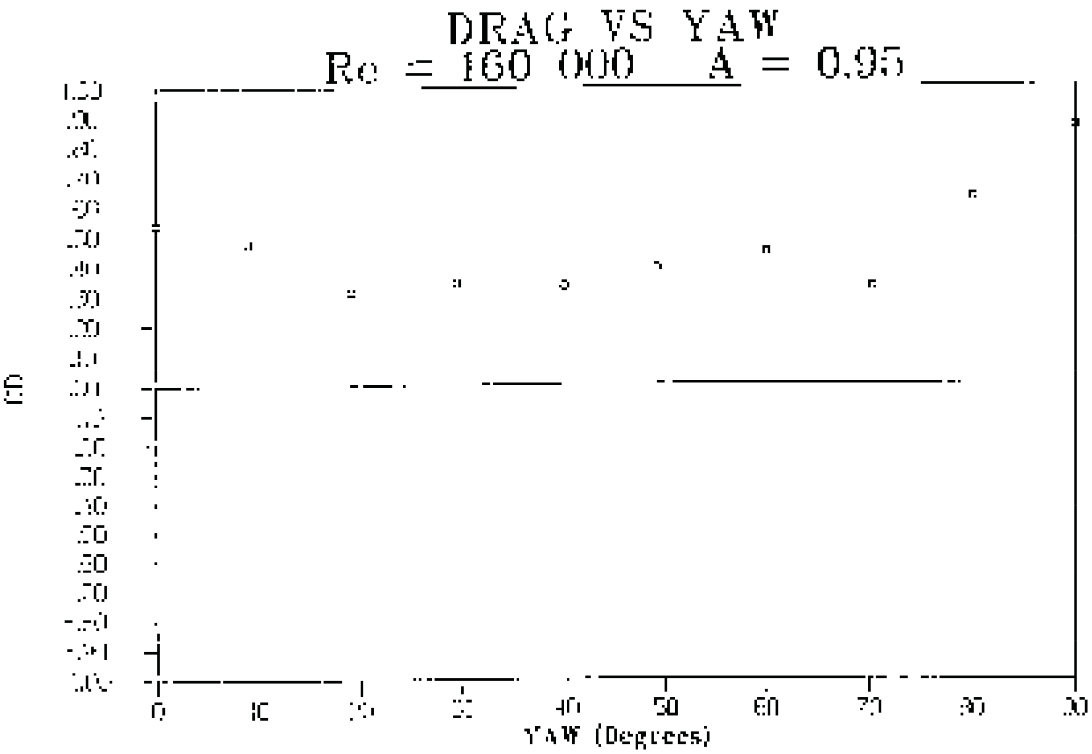

Fig 7.31. Drag vs Yaw angle for Re = 160 000 and the velocity ratio A = 0,95 using support B in position 2.

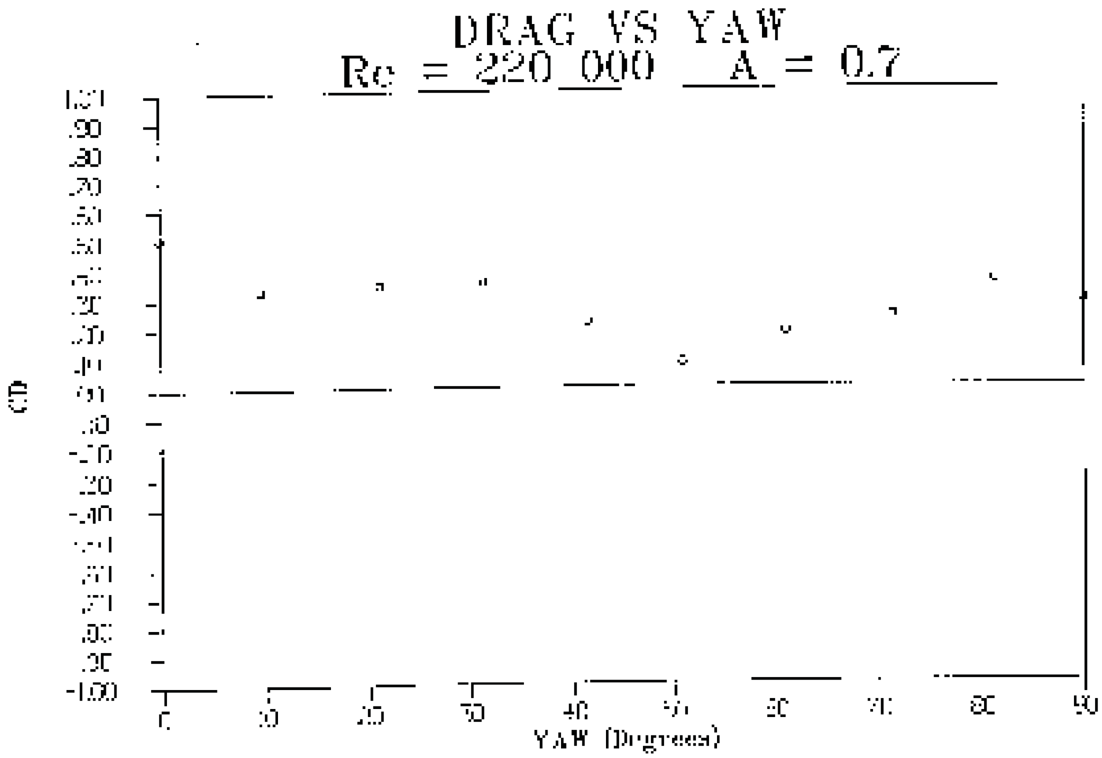

Fig 7.32. Drag vs Yaw angle for Re = 220 000 and the velocity ratio A = 0.7 using support B in position 2.

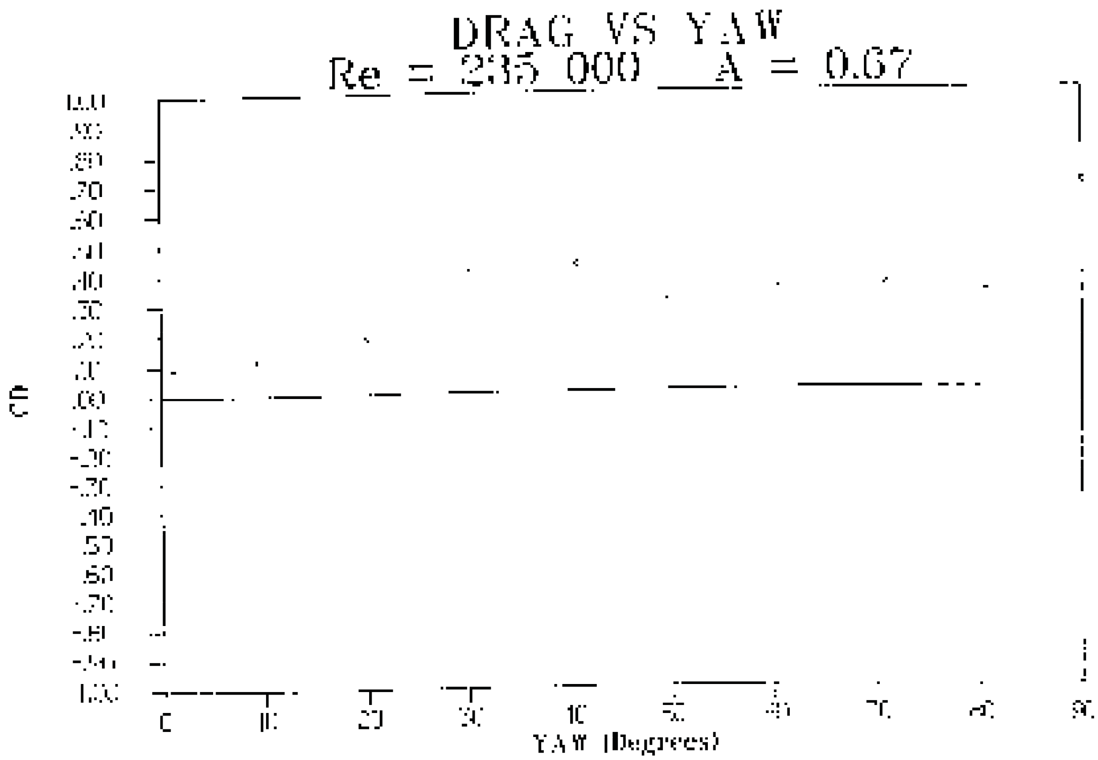

Fig 7.33. Drag vs Yaw angle for Re = 235 000 and the velocity ratio A = 0.67 using support A in position 2.

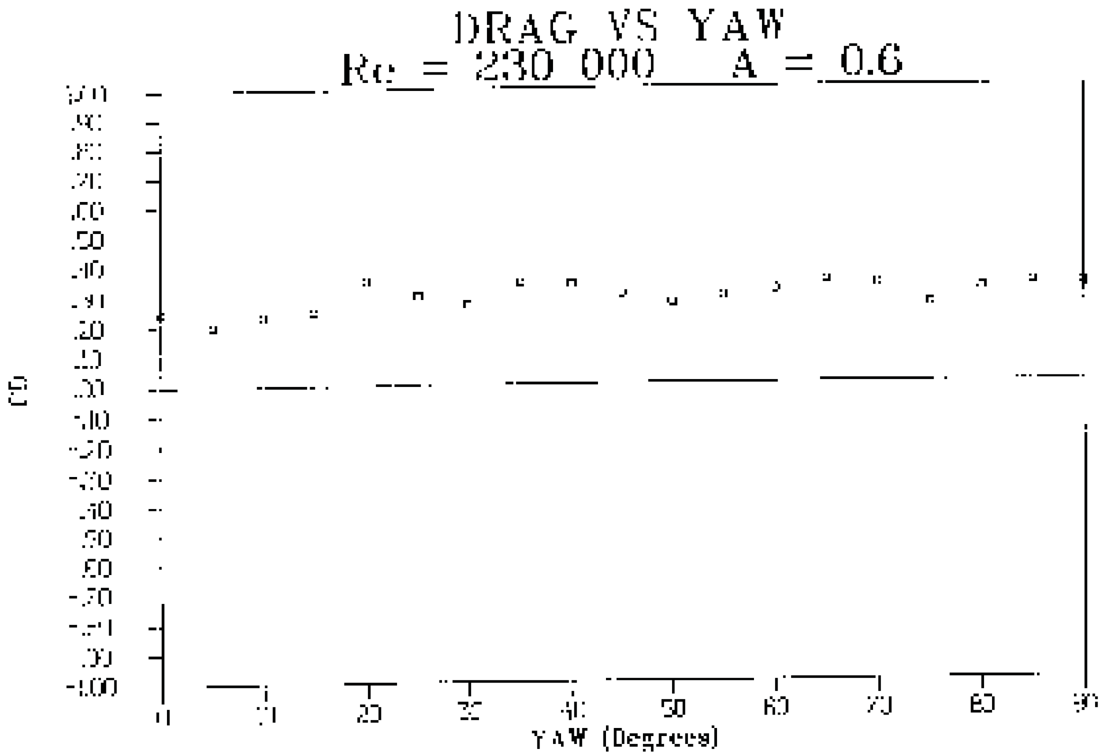

Fig 7.34. Drag vs Yaw angle for Re = 230 000 and the velocity ratio A = 0.6 using support C in position 2.

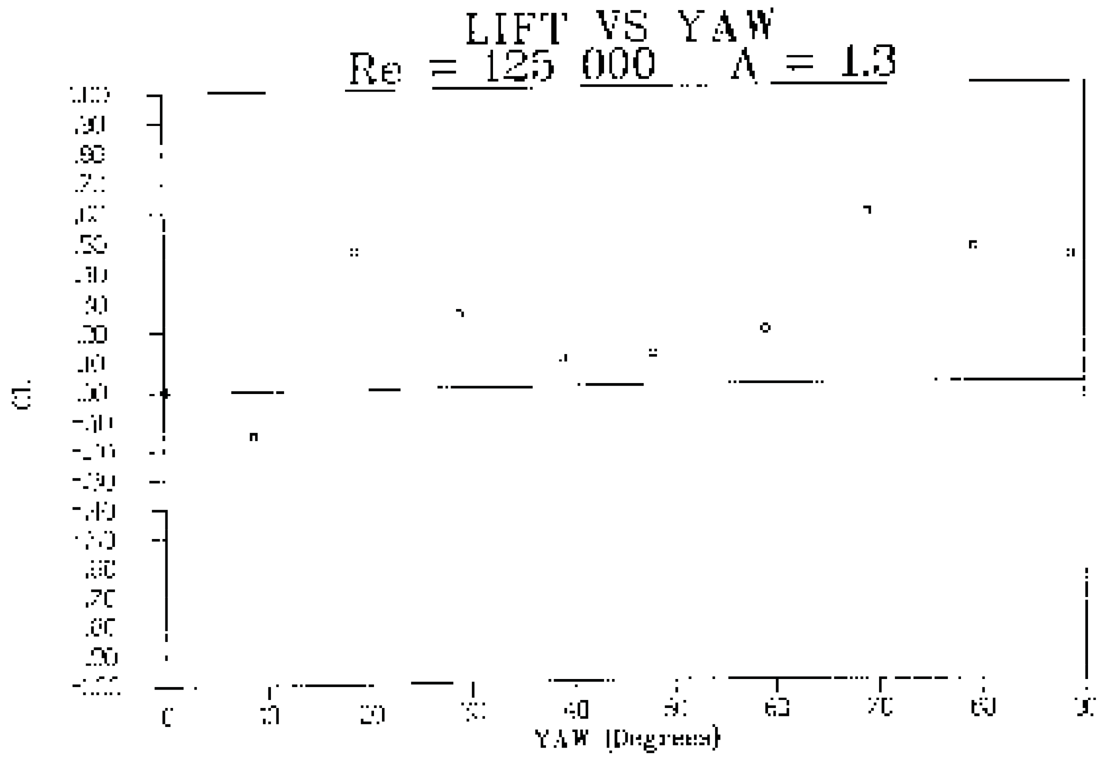

Fig 7.35. Lift vs Yaw angle for Re = 125 000 and the velocity ratio A = 1.3 using support A in position 1.

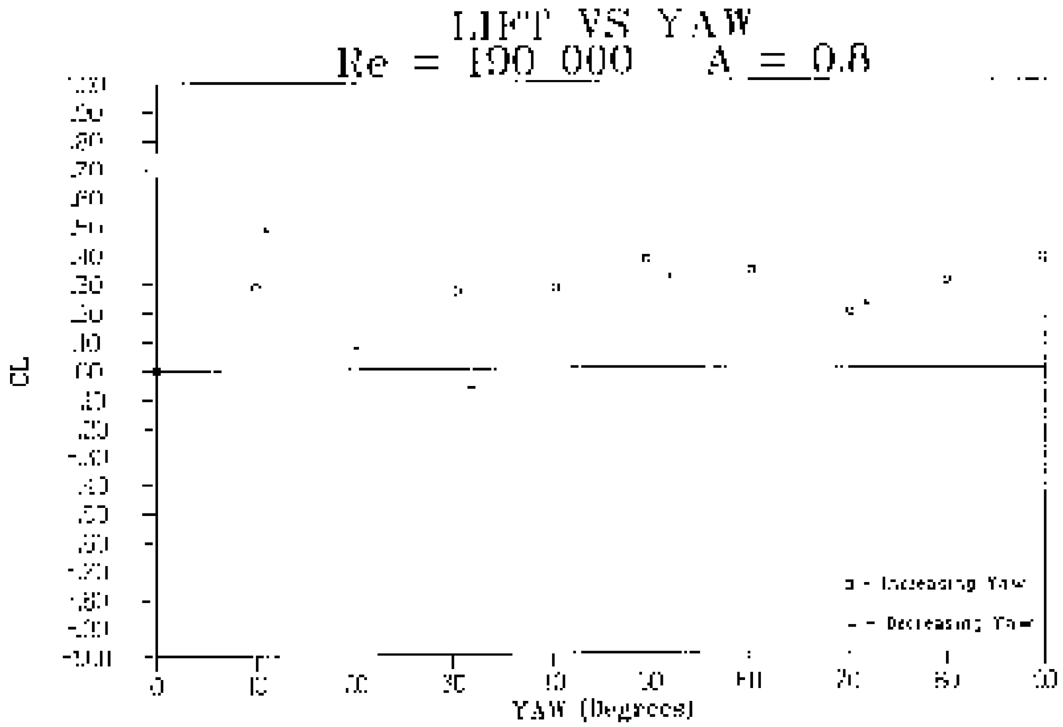

Fig 7.36. Lift vs Yaw angle for Re = 190 000 and the velocity ratio A = 0.8 using support A in position 1.

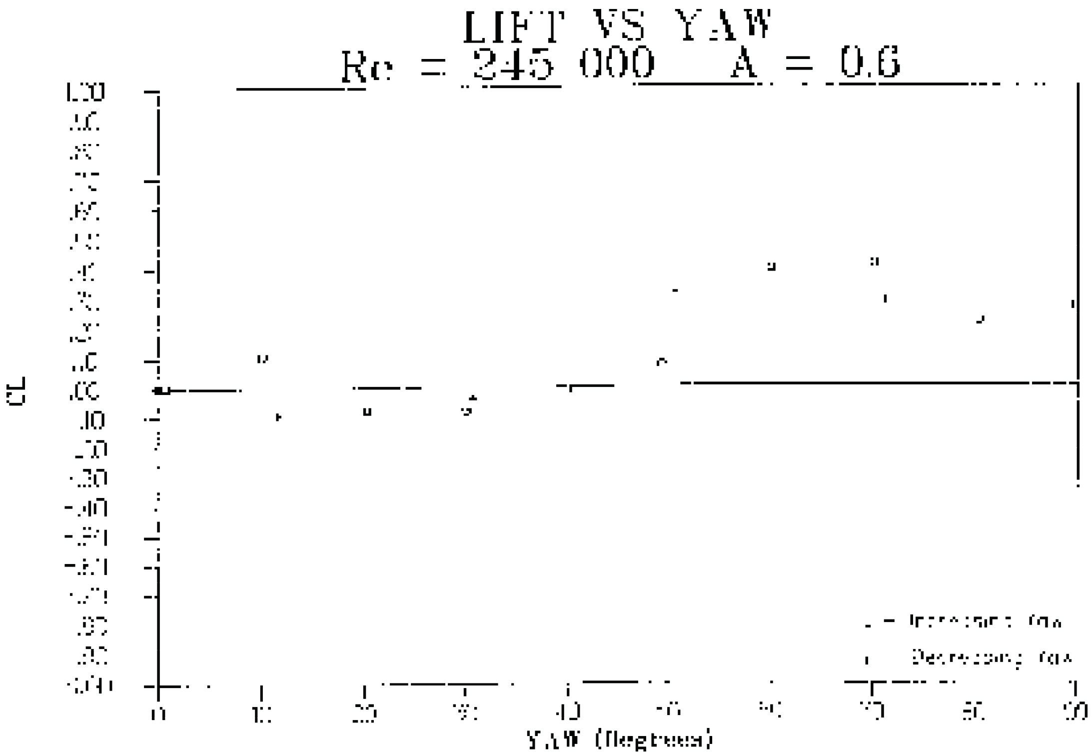

Fig 7.37. Lift vs Yaw angle for Re = 245 000 and the velocity ratio A = 0.6 using support A in position 1.

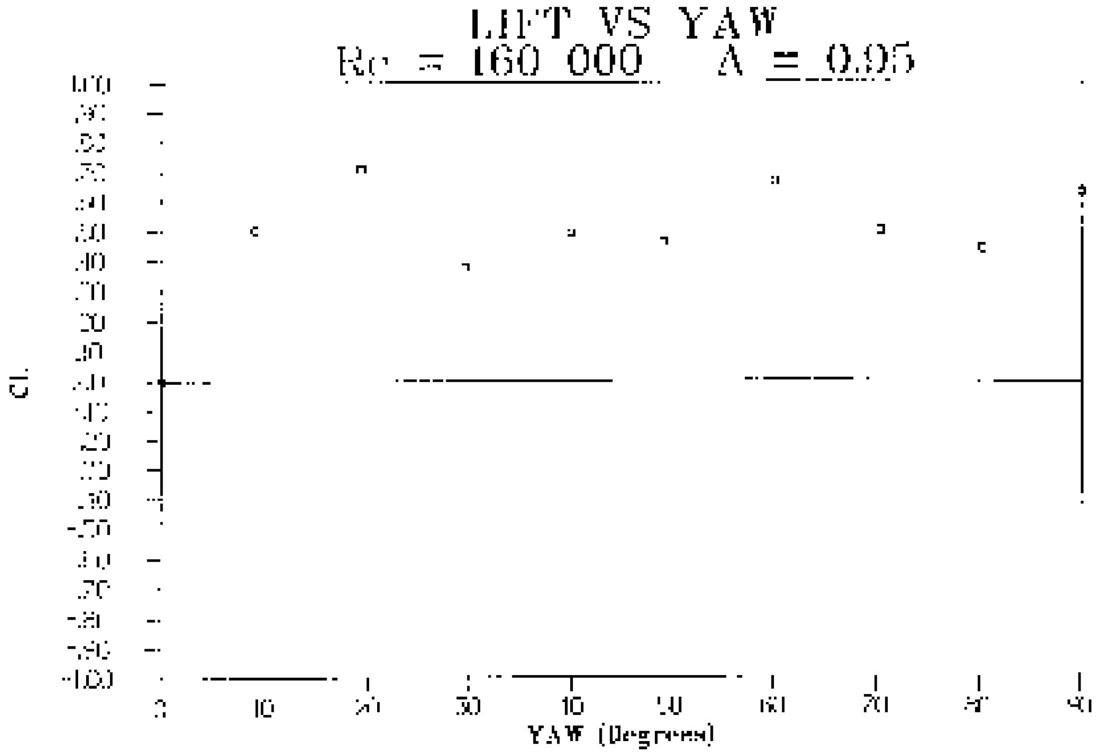

Fig 7.38. Lift vs Yaw angle for Re = 160 000 and the velocity ratio A = 0.95 using support B in position 2.

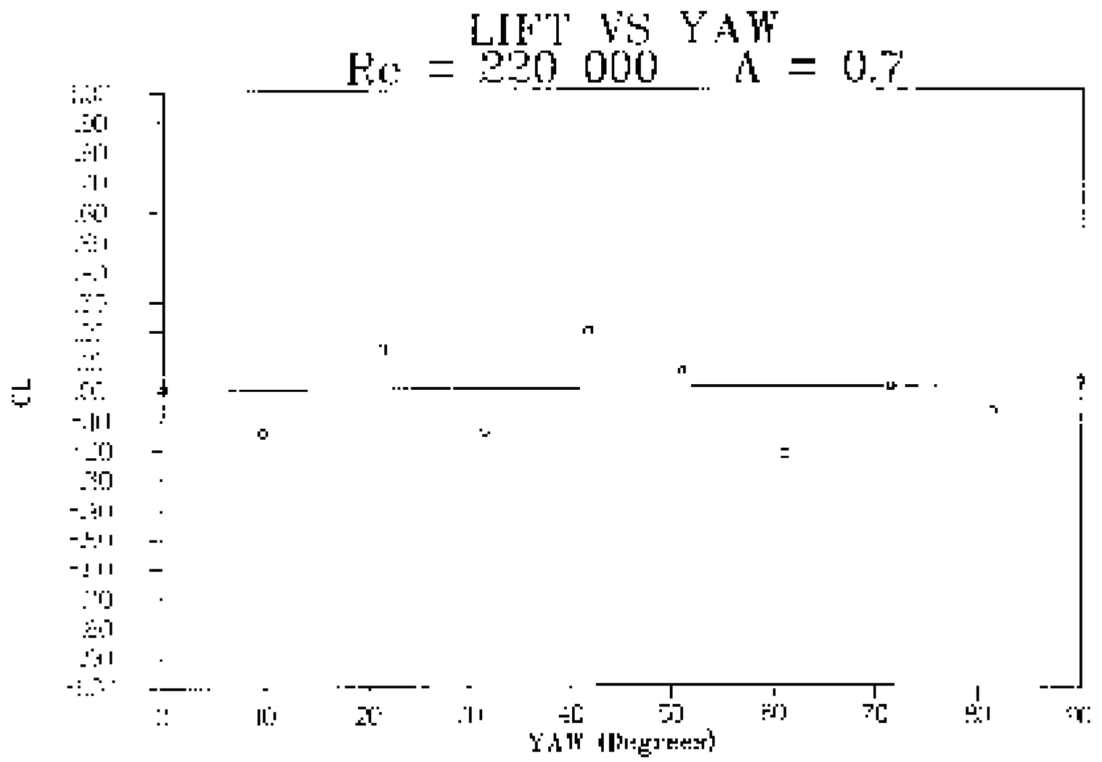

Fig 7.39. Lift vs Yaw angle for Re = 220 000 and the velocity ratio A = 0.7 using support B in position 2.

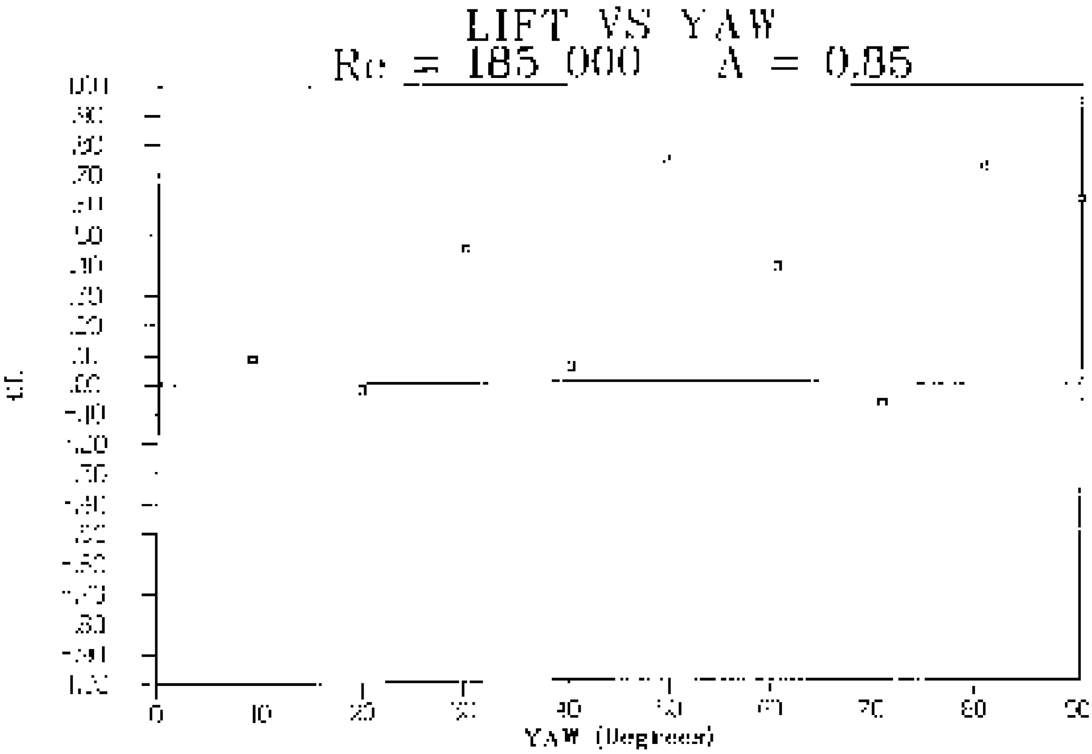

Fig 7.40. Lift vs Yaw angle for Re = 185 000 and the velocity ratio A = 0.85 using support A in position 2.

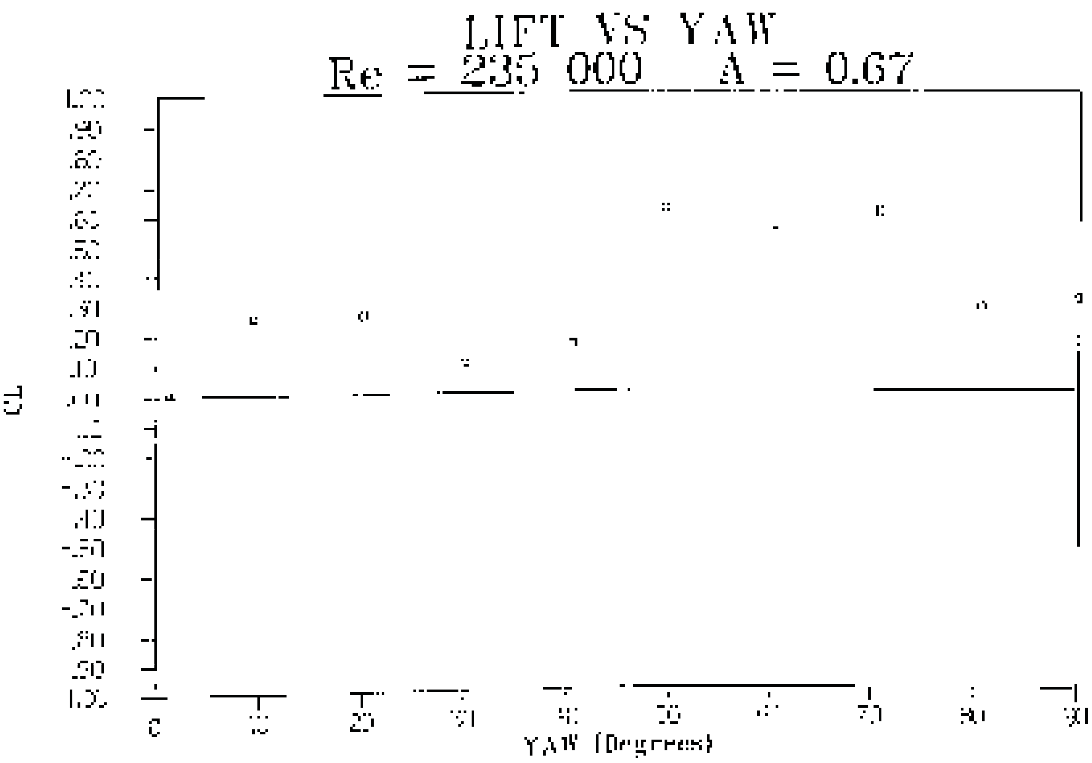

Fig 7.41. Lift vs Yaw angle for Re = 235 000 and the velocity ratio A = 0.67 using support A in position 2.

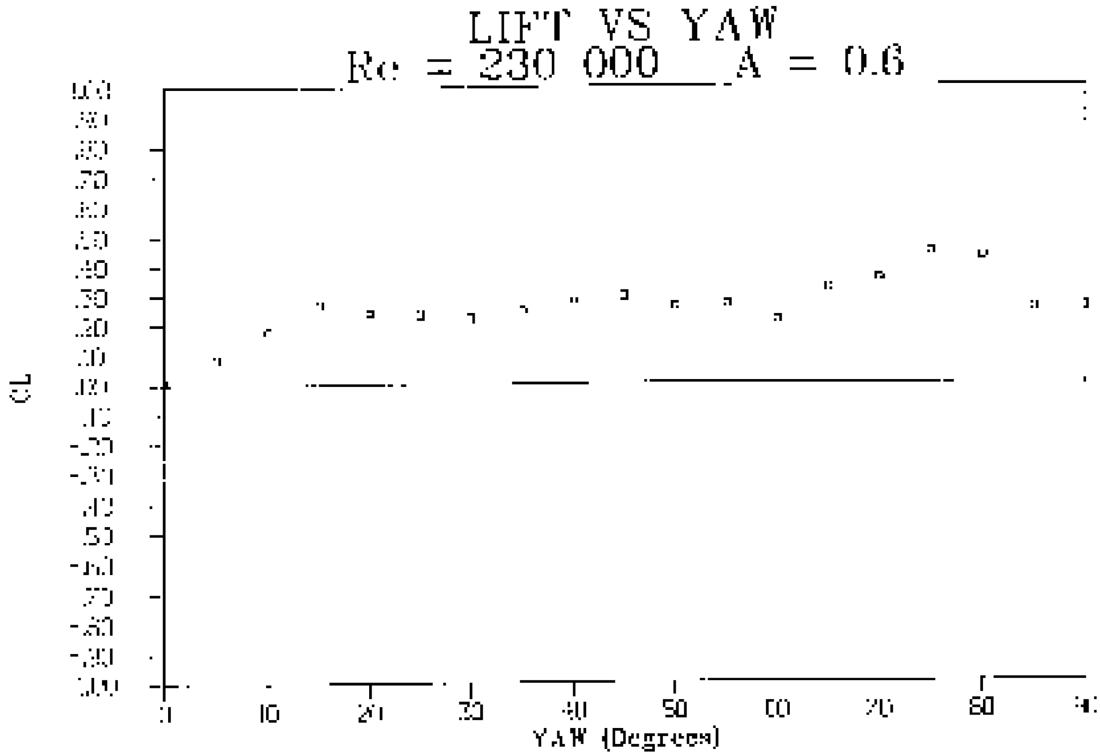

Fig 7.42. Lift vs Yaw angle for Re = 230 000 and the velocity ratio A = 0.6 using support C in position 2.

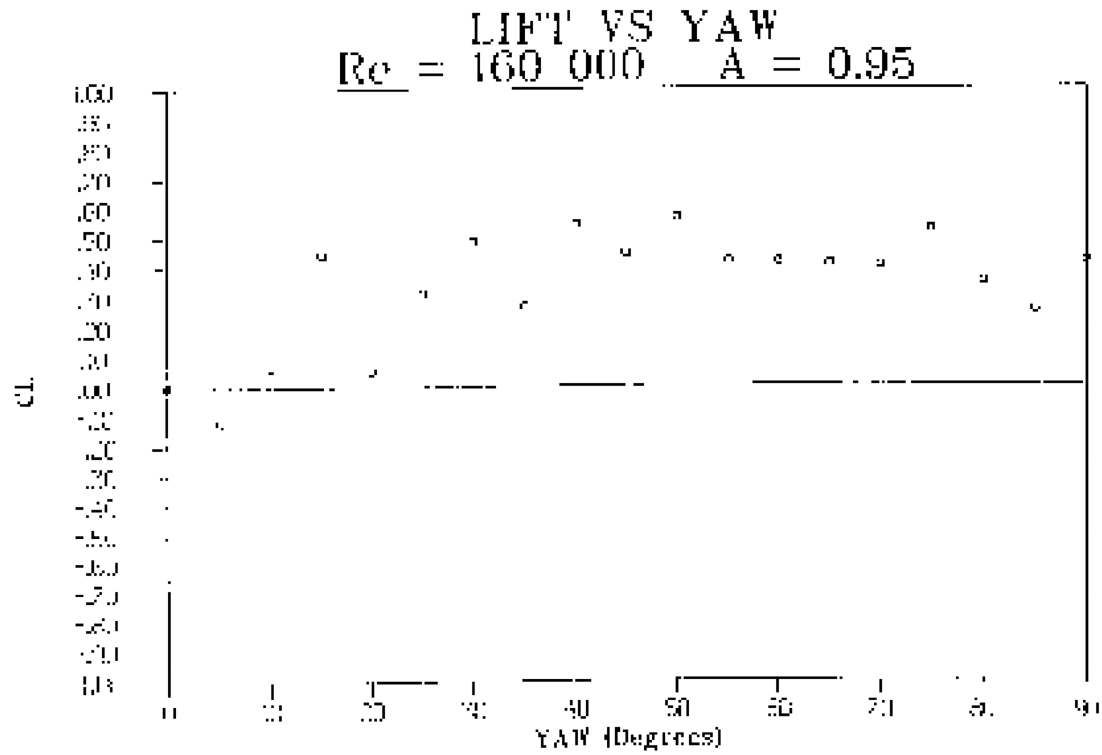

Fig 7.43. Lift vs Yaw angle for Re = 160 000 and the velocity ratio A = 0.95 using support C in position 2.

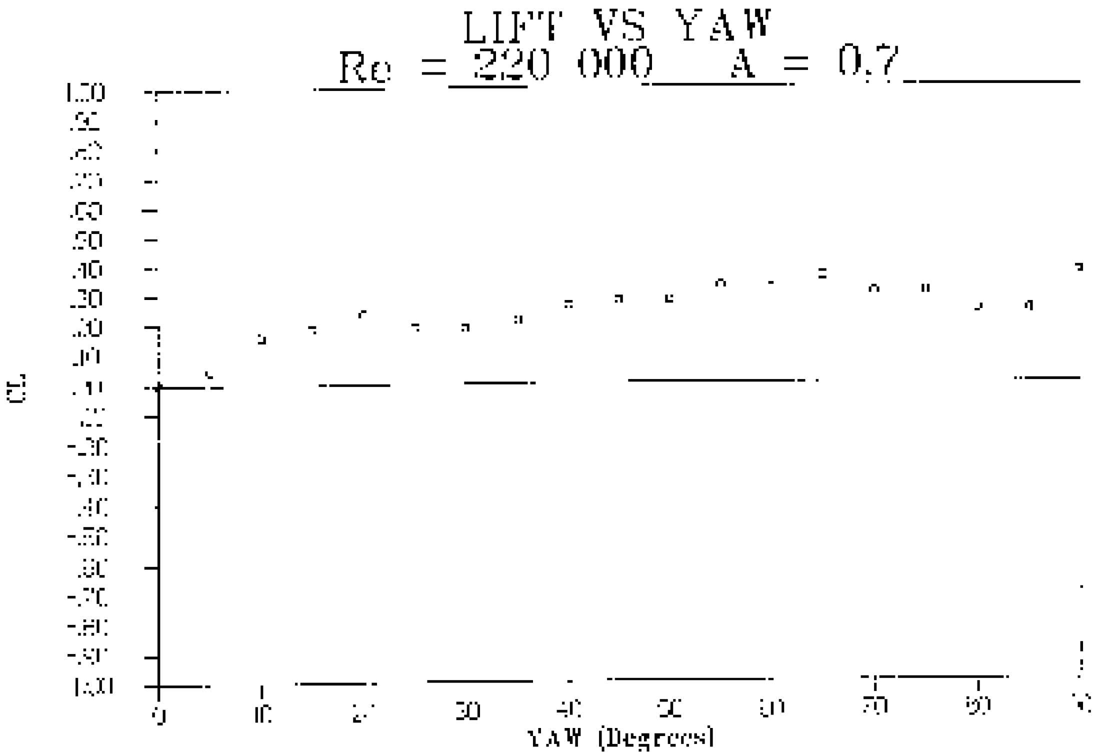

Fig 7.44. **Lift** vs Yaw angle for Re = 220 000 and the velocity ratio A = 0.7 using support C in position 2.

7.5 VARIATION OF DRAG WITH SPIN PARAMETER FOR FLOW PARALLEL TO SPIN AXIS

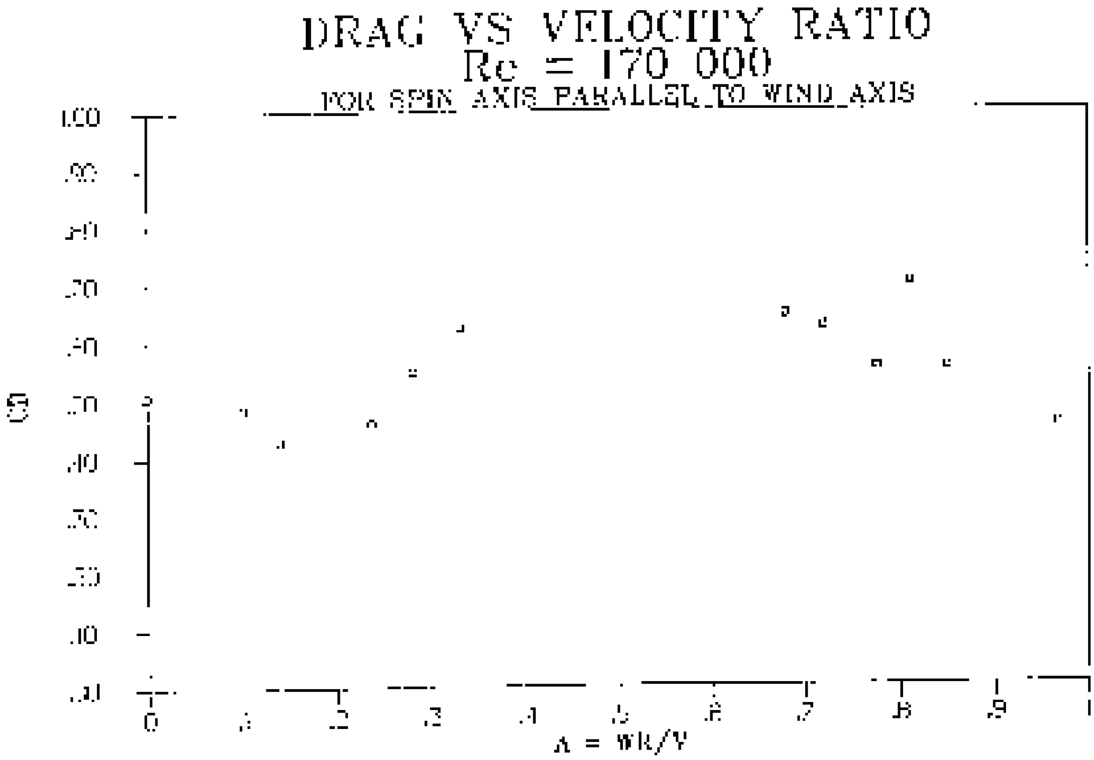

Fig 7.45. Drag vs velocity ratio for Re = 170 000 using support A in position 1.

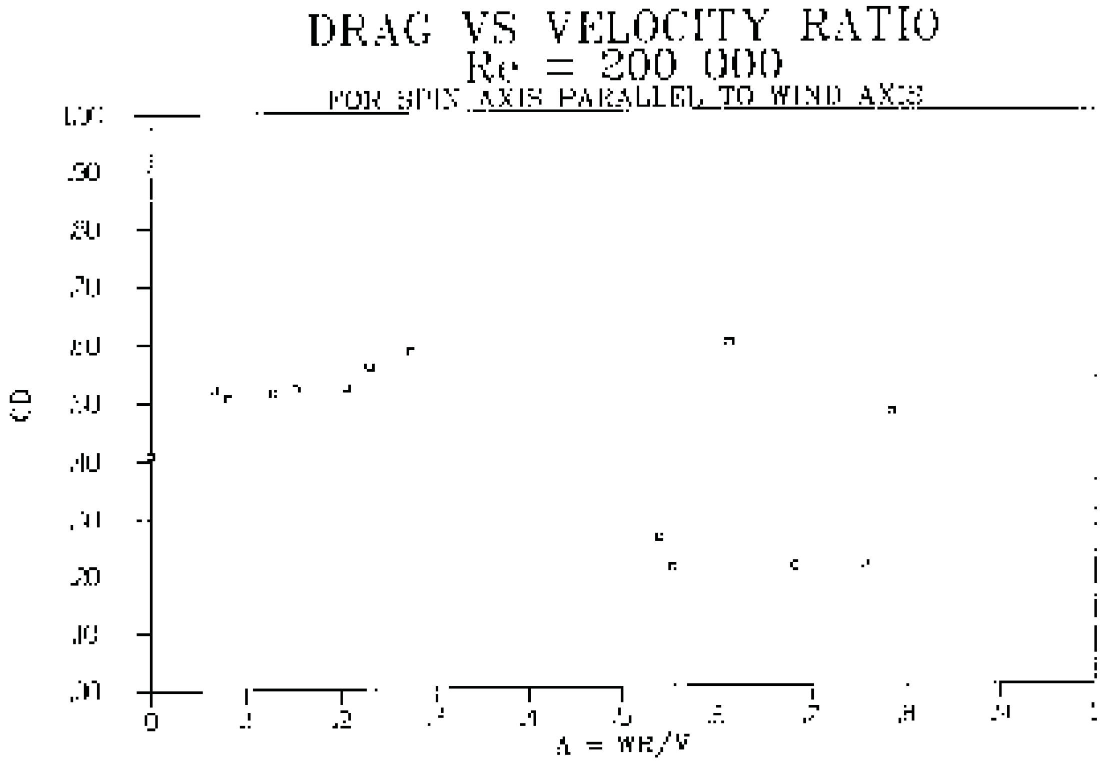

Fig 7.46. Drag vs velocity ratio for Re = 200 000 using support A in position 1.

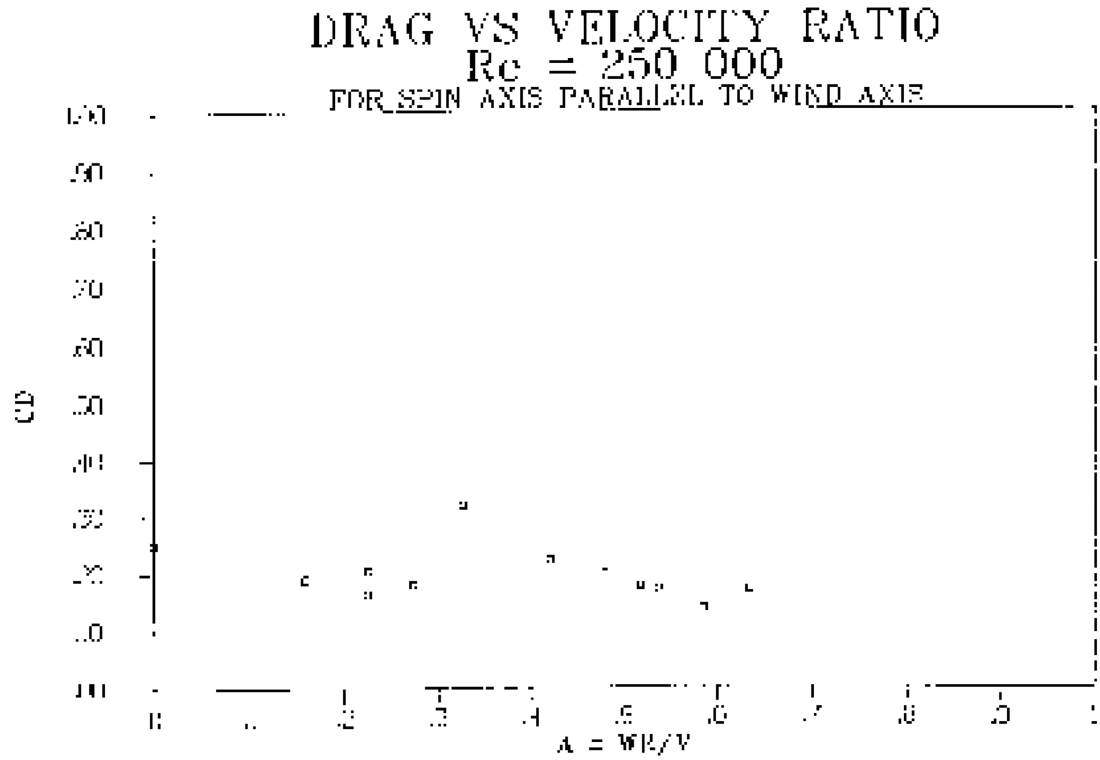

Fig 7.47. Drag vs velocity ratio for Re = 250 000 using support A in position 1.

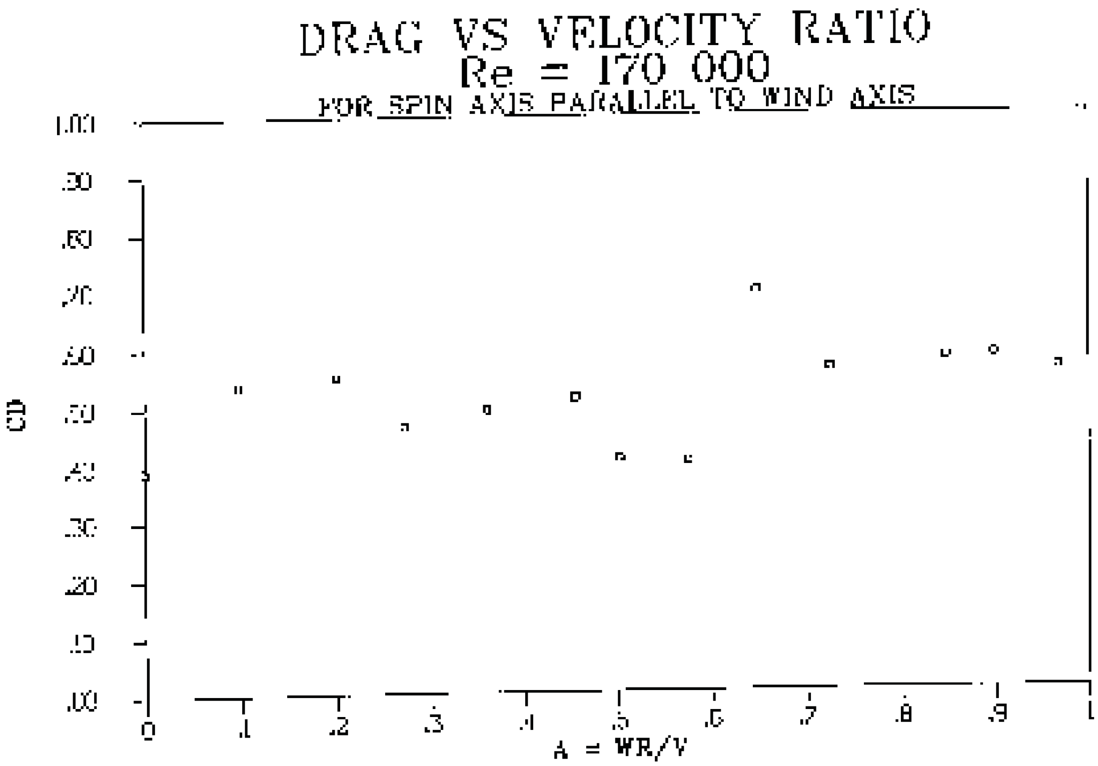

Fig 7.48. Drag vs velocity ratio for Re = 170 000 using support B in position 2.

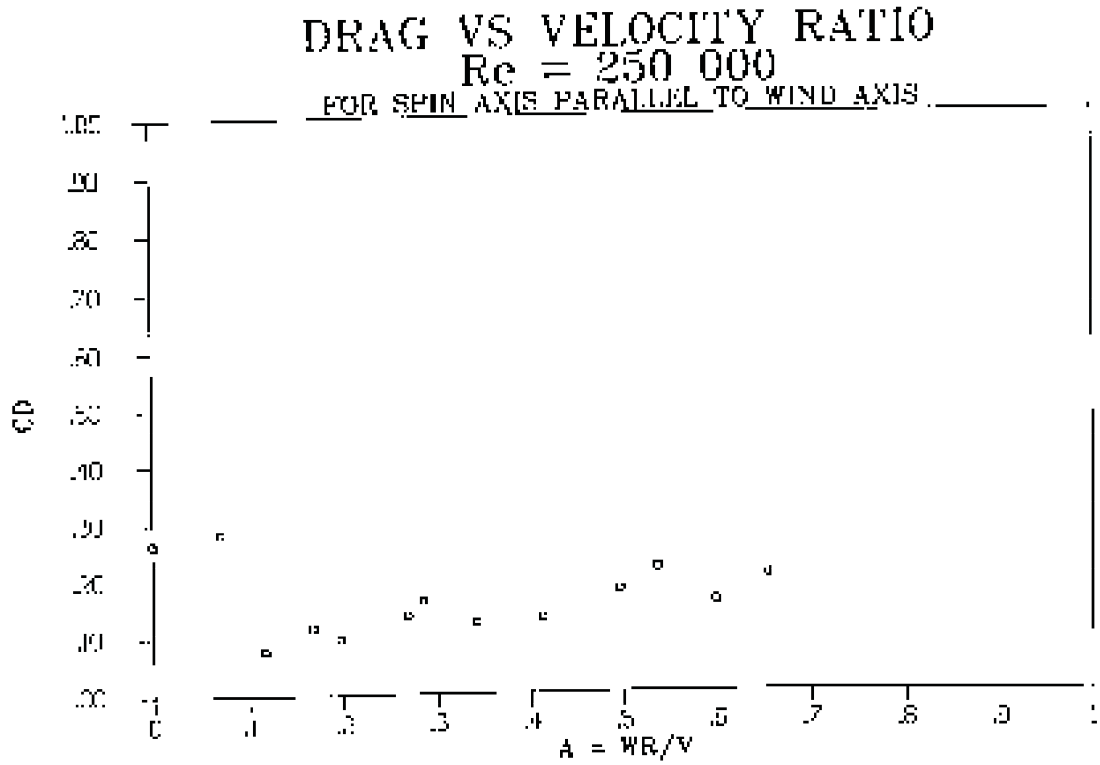

Fig 7.49. Drag vs velocity ratio for Re = 250 000 using support B in position 2.

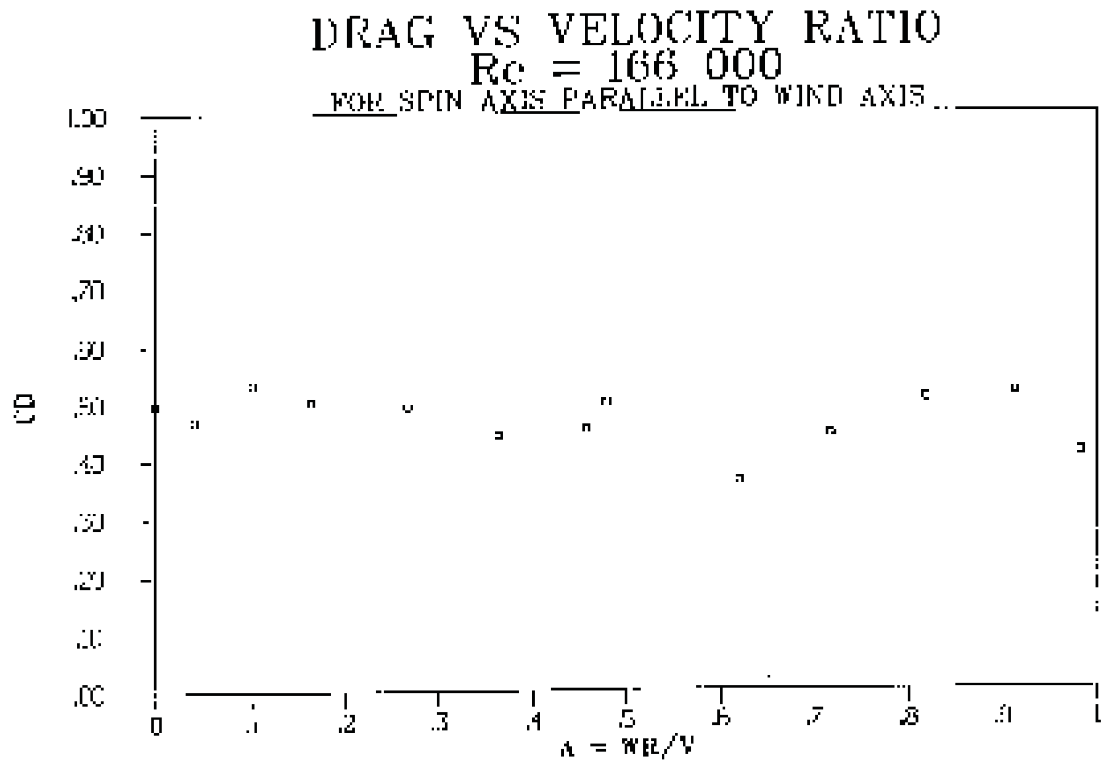

Fig 7.50. Drag vs velocity ratio for Re = 166 000 using support A in position 2.

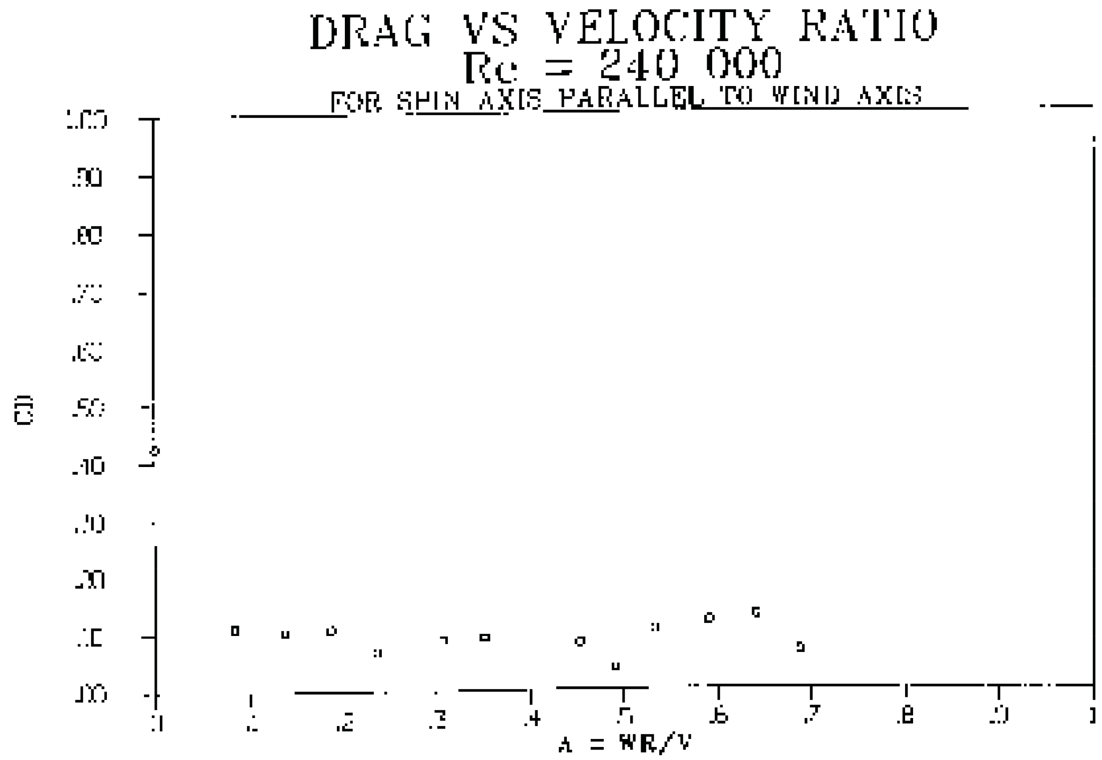

Fig 7.51. Drag vs velocity ratio for Re = 240 000 using support A in position 2.

7.6 PREDICTED VARIATION OF LIFT VS YAW ANGLE

The prediction of Lift variation with Yaw angle involved determining the effective velocity ratio for a given Yaw angle. The corresponding Coefficient of Lift was then taken from the relevant experimental test and used as the Lift for those given conditions. To simplify this, a third order polynomial was fitted to the experimental data for the given Reynolds number. The following section has a comparison of the experimental data and fitted data with its corresponding equation. The section following that shows the predicted curves.

There will only be three cases predicted and they are:

Re = 70 000	A = 0.6
Re = 165 000	A = 0.95
Re = 230 000	A = 0.6

7.6.1 FITTING A THIRD ORDER POLYNOMIAL EQUATION

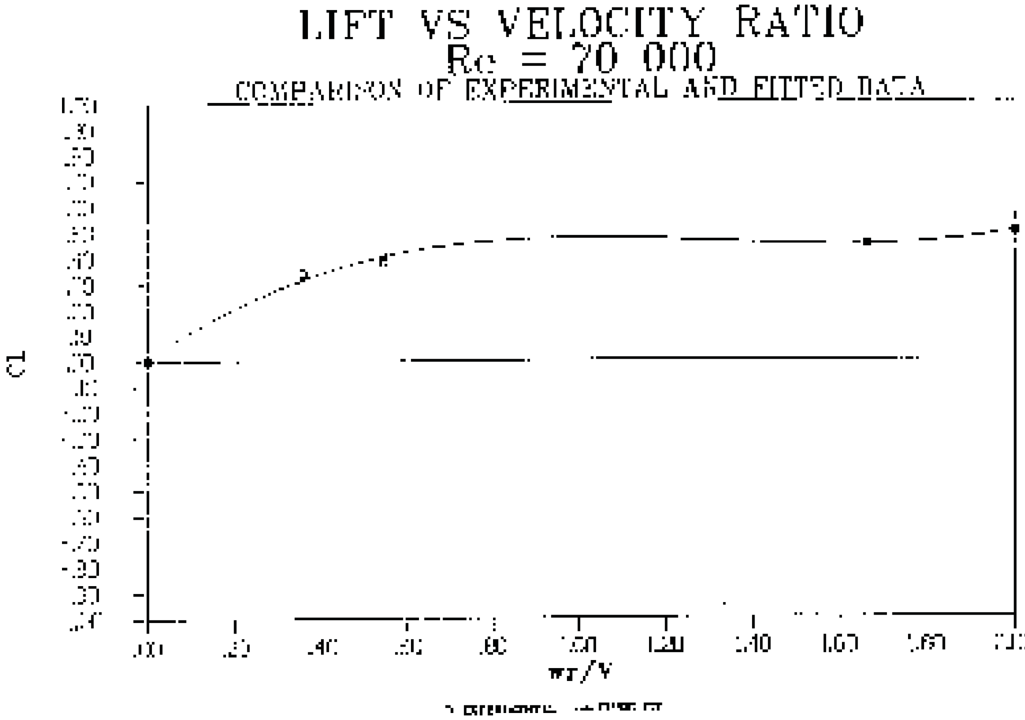

Fig 7.52. Comparison of experimental and fitted data for Re = 70 000.

$$y = 0.00591 + 1.18272x - 0.94288x^2 + 0.23589x^3$$

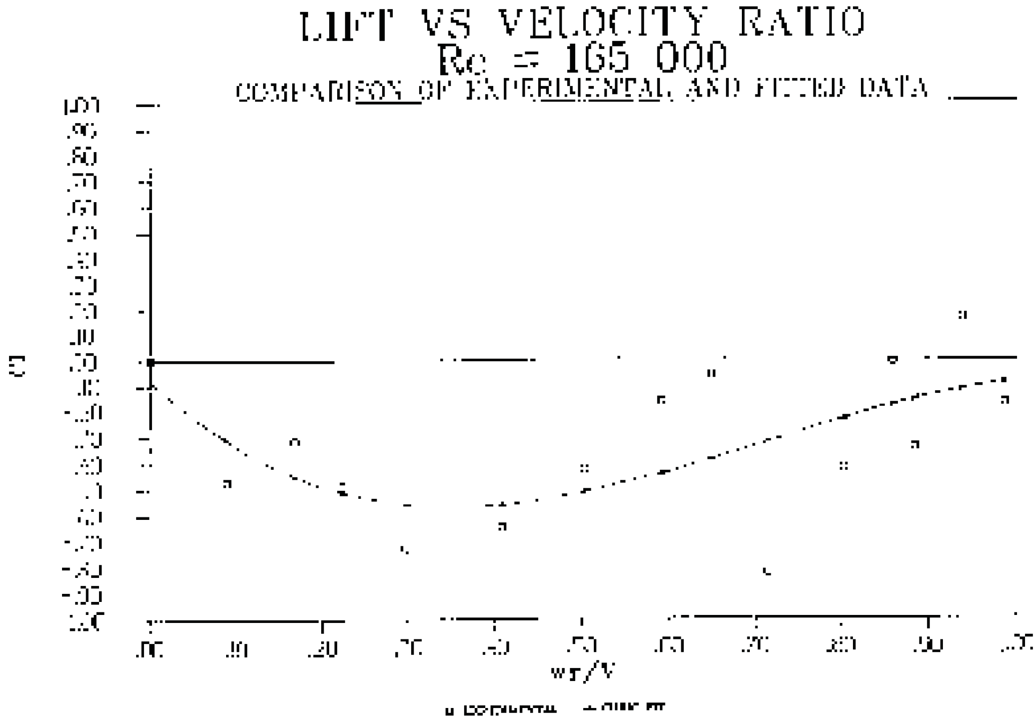

Fig 7.53. Comparison of experimental and fitted data for Re = 165 000.

$y = -0.08196 - 3.07203x + 5.74265x^2 - 2.67002x^4$

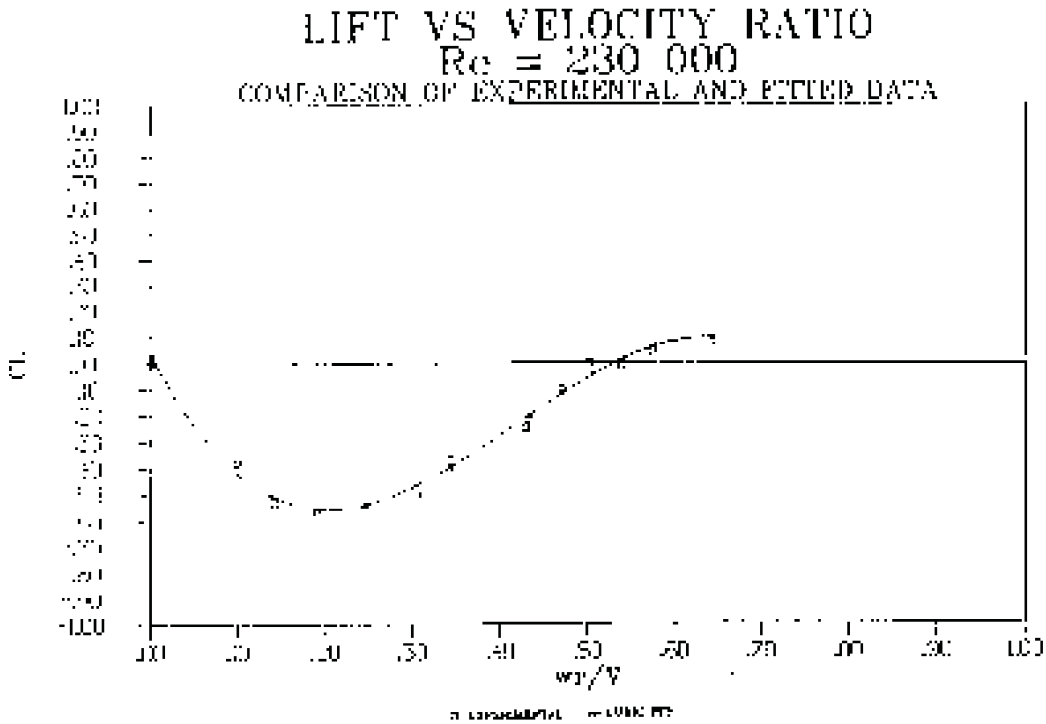

Fig 7.54. Comparison of experimental and fitted data for Re = 230 000.

$$y = 0.02460 - 6.35152x + 20.46212x^2 - 16.18783x^3$$

7.6.2 PREDICTED VARIATION OF LIFT WITH YAW ANGLE

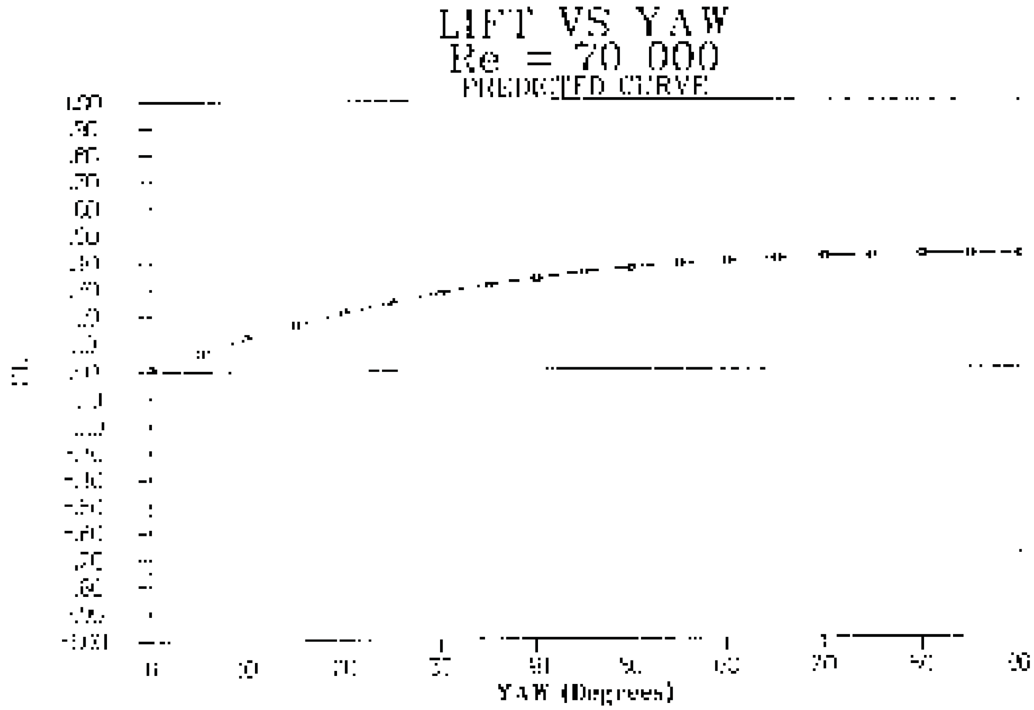

Fig 7.55. Predicted variation of Lift with Yaw angle for Re = 70 000.

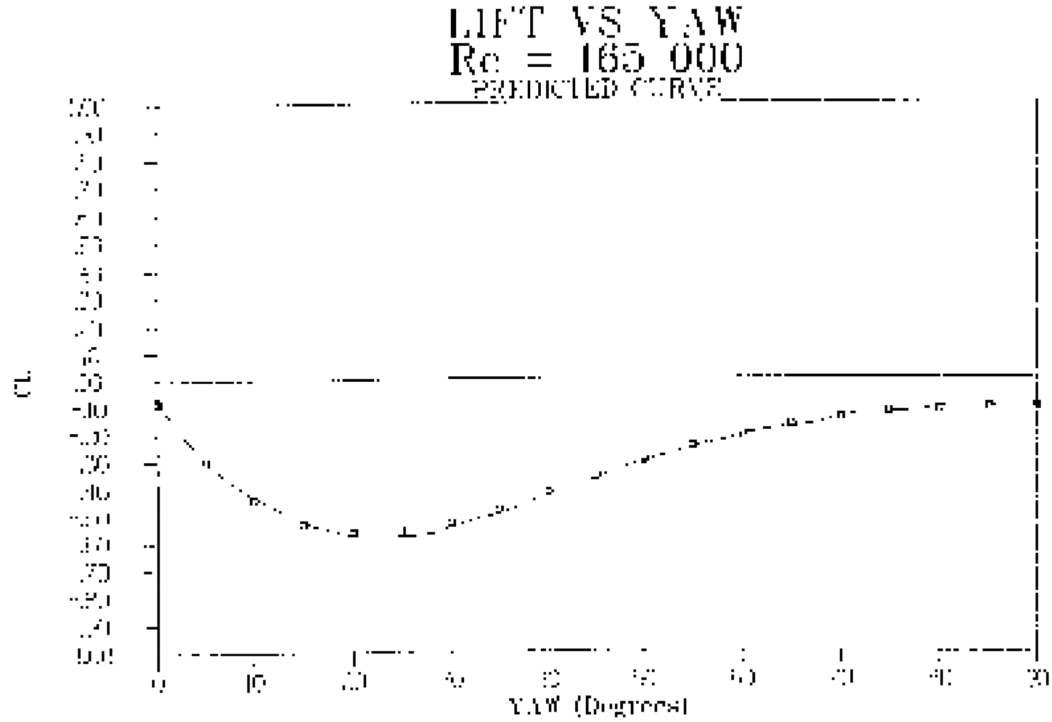

Fig 7.56. Predicted variation of Lift with Yaw angle for Re = 165 000.

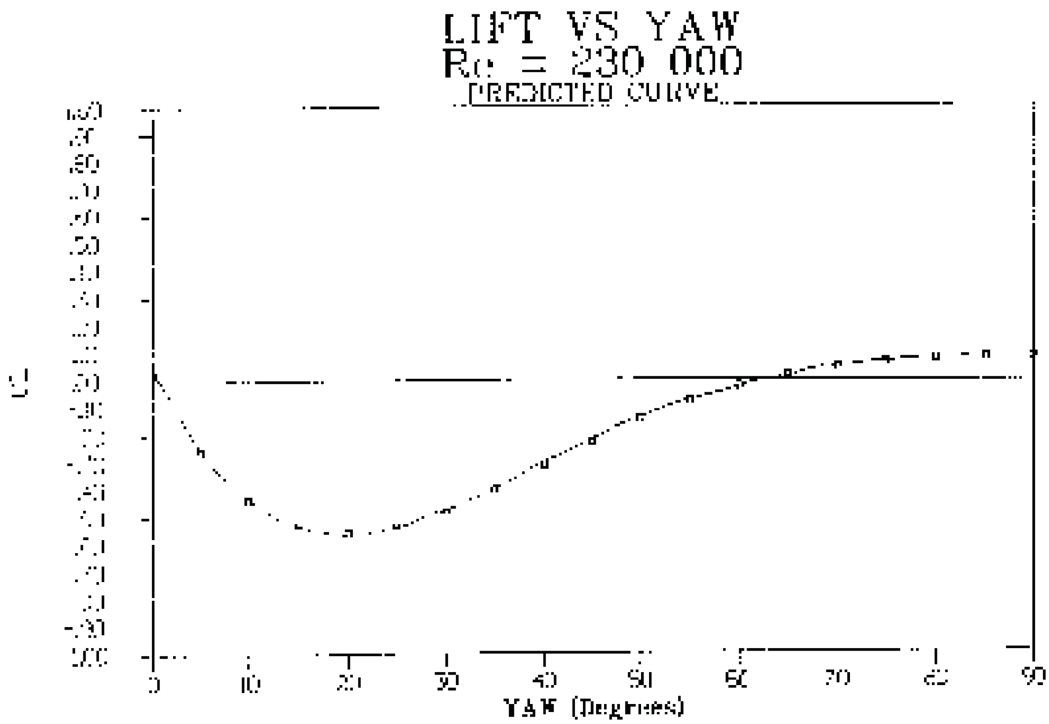

Fig 7.57. Predicted variation of Lift with Yaw angle for Re = 230 000.

8 DISCUSSION

The experimental equipment used for these tests was as yet unused. Some of this equipment had been built in house and that which hadn't, had been supplied without the proper documentation. It is for these reasons that the reliability of the equipment had to be ascertained. To do this it was decided to re-calibrate the sting balance.

The sting was mounted on three different types of support system. The reason for the three independent supports was that this would indicate if the source of readings that did not conform to the published data was due to the support or to actual aerodynamic effects. The first support used was a parallelogram support. It had its long uprights made out of slender stainless steel tubing, pin jointed to facilitate pivoting. This however appeared to be unstable. The second system had shorter uprights welded to a base plate. This system was much more rigid. The third system was even stiffer than the first two. It comprised a vertical tube welded to a base plate, held in place by two angled struts. This support was used for the third series of tests carried out after the sting was repaired. At this time the turn-table was in use for other experimentation, and therefore a support was required that could facilitate changing Yaw angles while the base was stationary.

If the calibration is referenced it can be seen that a plot is given of applied and measured load for each loading case. The software carrying out the multiple linear regression was limited to a total of 550 sets of readings when comparing six independent variables to a dependant one. It was felt, since under most test conditions the balance is loaded with more than one component, the calibration should be carried out with the loading as comprehensive as possible, even if this meant that fewer sets of readings could be taken per loading condition. For this reason the calibration was limited to four readings per loading case. The calibration matrix takes into account cross linking to the first order as this is the accepted practice unless very small tolerances are required.

When one considers the case of a two dimensional cantilever, the force perpendicular to the beam at the root can only be changed by changing the applied load. The moment resulting from this load can be changed by changing the load or the point of application. It is for this reason that when calibrating the sting the complete range of loads was applied at each station. The design of the sting should have rendered such loading unnecessary but it was felt that the cross linking resulting from small displacements and misalignments warranted it.

The calibration matrix should have been a 6x6 matrix with zeros in all positions not on the main diagonal. When the balance was calibrated the first time it was found that columns two and three required swapping as did columns five and six. Apart from this there was a slight misaligment about the axis of the sting. After accounting for these errors the cross linking was of the order of 5%.

The tare (measuring the load on the sting while the tunnel is running without a model mounted) after this calibration showed that the Z component corresponding to Lift had an unacceptably high value. The tare was found to be independent of wind velocity as increases occurred at an arbitrary angle of Yaw, and when the same test was carried out for different angles of attack the tare value was always positive. This implied that the zero value was changing when the balance was being moved. Although the change was not happening every time it is reasonable to conclude that the zero was drifting. A loose connection or fault in the glueing of the strain gauges would only result in a drift of zero if the movement was sufficiently rapid to jar the sting. For this reason it was deemed necessary to repeat the tests already carried out once, with the sting rotated through 90° about its longitudinal axis . This would result in the component whose accuracy was questionable measuring side force and not Lift, the component of most interest.

The calibration matrix generated after the sting was rotated had the largest coefficients along the main diagonal. The order of magnitude of cross linking was once again 5%.

Tare tests were carried out with the motion of the sting being as smooth as possible. The result of this caution is clearly visible in the graphs. This strengthens the theory that the balance had a fault in the component originally used for Lift.

The graph of applied load versus measured load after rotation (position 2) shows that the Y component (previously the Z component) was still the cause of errors.

The sting was sent in for repairs and a noticeable improvement was evident. Further testing was carried out. This third series of tests was limited to those tests requiring all three force components, namely Lift and Drag variation with changing Yaw angle.

The UPM 60 does have an occasional drift. This can be seen when one reading for a particular loading condition is not consistent with the other three. It was for this reason that a minimum of eight readings were taken for each loading case during testing. These results were then averaged to give one set of results per test.

8.1 DRAG VS REYNOLDS NUMBER

The Drag tests were carried out to ascertain the reliability of the sting and support under test conditions. This test was chosen as there is a lot of published data of Drag versus Reynolds number. If one puts the results published in the text books on the same set of axes the scatter of C_D will range from 0.35 to 0.55 (Schlichting, Mc Cormick and Massey) (Fig. 3.1).

The experimental results (Fig. 7.1 & Fig. 7.2) were within this range except for a few stray points. The other noticeable item is that the scatter is greater for the sting perpendicular to the flow than for the sting parallel to the flow. Two reasons for this can be suggested. The first is that the support is not as stiff in the direction of the flow as when rotated to an angle of Yaw of 90^0. The second is that the sting trips the flow over the sphere causing vortices to be shed unevenly resulting in an uneven Drag trace. It was not determined which of these effects was the greater cause of scatter.

The support was tied down to determine whether the cause of the scatter was flexibility of the support (Fig. 7.3). The results of this test were far better than those done previously. The scatter was only between C_D = 0.45 and C_D = 0.55. The test also showed a critical Reynolds number of about 225 000. The critical Reynolds number is defined in Rae and Pope (1984) as being when the value of C_D drops past the 0.3 level. The critical Reynolds number for a sphere in low turbulence wind is Re = 385 000. This display of transition is disturbing.

The support was then replaced with a solid steel support bolted to the floor. At the same time the sting was rotated since the faulty component was noticed and a complete set of tests had been completed. After rotating the sting it must be realised that the results of a Drag test at 90^0 would be questionable. This meant that tests were only performed with the sting parallel to the flow. The results of this test showed a scatter of C_D between 0.4 and 0.55 (Fig. 7.4). The results do show a drop in C_D at Re = 225 000 but this was not sufficient to call critical.

8.2 TUNNEL TURBULENCE

Massey (1979) gives a plot displaying the deviation of critical Reynolds number due to turbulence and distortion (Fig. 3.2). The tolerances on the dimensions were within 1% which would result in minimal deviation in critical Reynolds number. The surface roughness was not significant implying that the drop in critical Reynolds number was due to turbulence. The critical Reynolds number of a sphere in free flight is 385 000.

Rae and Pope (1984) and Schlichting (1979) both quote the method developed by Dryden of scaling the Reynolds number and measuring the turbulence by means of the experimentally obtained critical Reynolds number.

When using the method described in Rae and Pope, one first finds a turbulence factor and then using a graph one can obtain the turbulence level. Schlichting's method on the other hand uses the critical Reynolds number to determine the turbulence level.

The critical Reynolds number was only reached in one test. The maximum Reynolds number obtained was 250 000. This was limited by the maximum velocity of the tunnel and the size of the sphere. The other tests carried out had not reached the critical stage by Re = 250 000. This implies that a very conservative estimate of the turbulence is that based on a critical Reynolds number of 225 000.

Using both methods as a check the turbulence level was determined to be 0.85% resulting in a turbulence factor of 1.71. The turbulence factor is simply the ratio of critical Reynolds number for the sphere in free flight to the critical Reynolds number of the sphere in the tunnel.

For a more realistic turbulence value one can assume that except for the test carried out with the parallelogram support tied down, the lowest that the critical Reynolds number could be is 250 000 which would result in a turbulence level of 0.65% and a turbulence factor of 1.54.

Rae and Pope in their book on Low Speed Wind Tunnel Testing (1984) state that developmental tunnels have turbulence levels as high as 0.5% in the axial direction. Only large government tunnels attempt to have turbulence levels as low as 0.1%.

If a smaller sphere is used then the true critical Reynolds number can be found, and it would be possible to determine if the level of turbulence is acceptable.